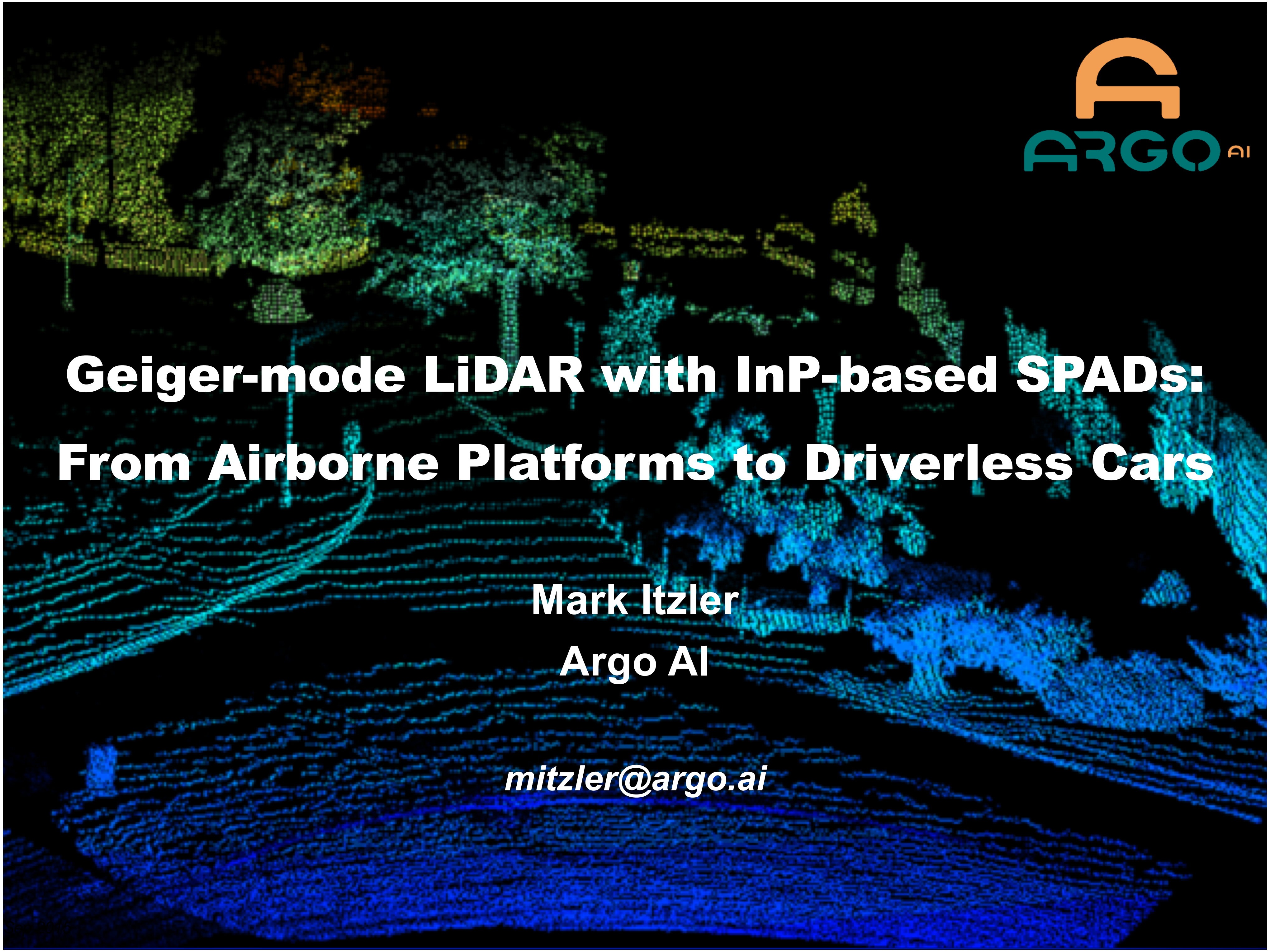

Geiger-mode LiDAR with InP-based SPADs: From Airborne Platforms to Driverless Cars

Mark Itzler
Argo AI

mitzler@argo.ai

Overview of Argo AI

Developing Virtual Driver System for Autonomous Vehicles

Founded by Bryan Salesky and Peter Rander in late 2016

Ford investment announced in Feb 2017

2 generations of cars built with Ford

Four office locations:

- Pittsburgh, Pennsylvania
- Dearborn, Michigan
- Mountain View, California
- Cranbury, New Jersey

Acquired Princeton Lightwave in Oct 2017

- In-house Geiger-mode LiDAR technology

Outline

Basics of InGaAs/InP SPADs

Device performance attributes

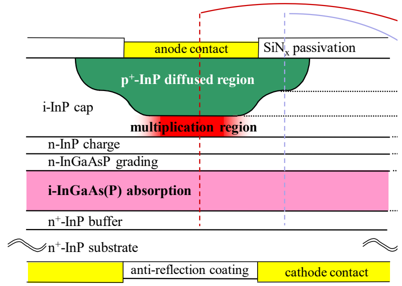

GmAPD cameras for airborne 3D LiDAR imaging

FPA integration and camera performance

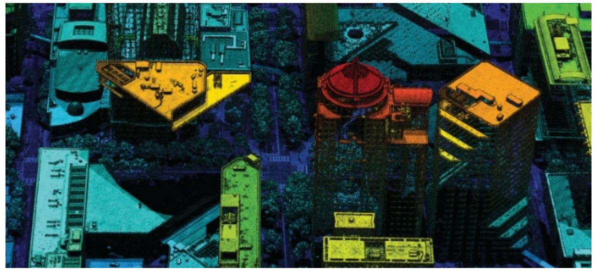

GmAPDs for 3D LiDAR in autonomous vehicles

Design considerations and demonstrator performance

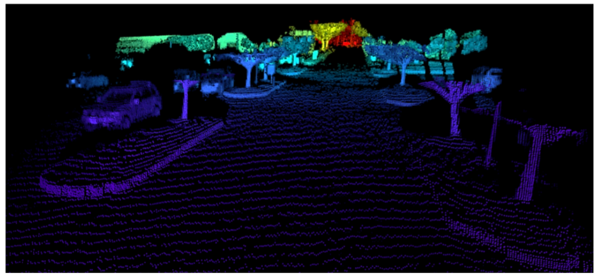

Why detect single photons in the SWIR?

Minimal loss in optical fiber (e.g., at 1.5 μm)

Covertness (to human vision and I^2 night vision goggles)

Reflective imaging (+ spectral information)

Greater eye safety for active imaging (beyond 1.4 μm)

Environmental factors

- Less solar background than visible/NIR
- Better atmospheric transmission

Technological factors

- Maturity of pulsed laser sources (e.g., 1.06 μm, 1.5 μm)
- Maturity of SWIR optics (e.g., from telecom)

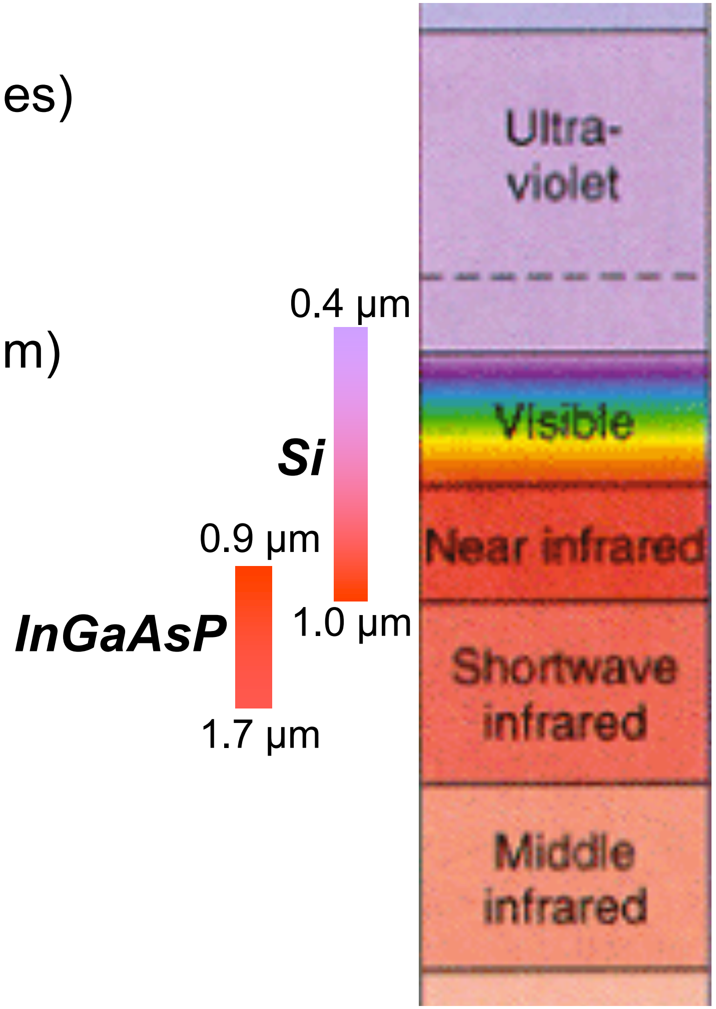

Single photon communications:
initial driver for InGaAs/InP SPADs

Exploit quantum mechanical nature of photons

quantum information processing (e.g., quantum cryptography and computing)

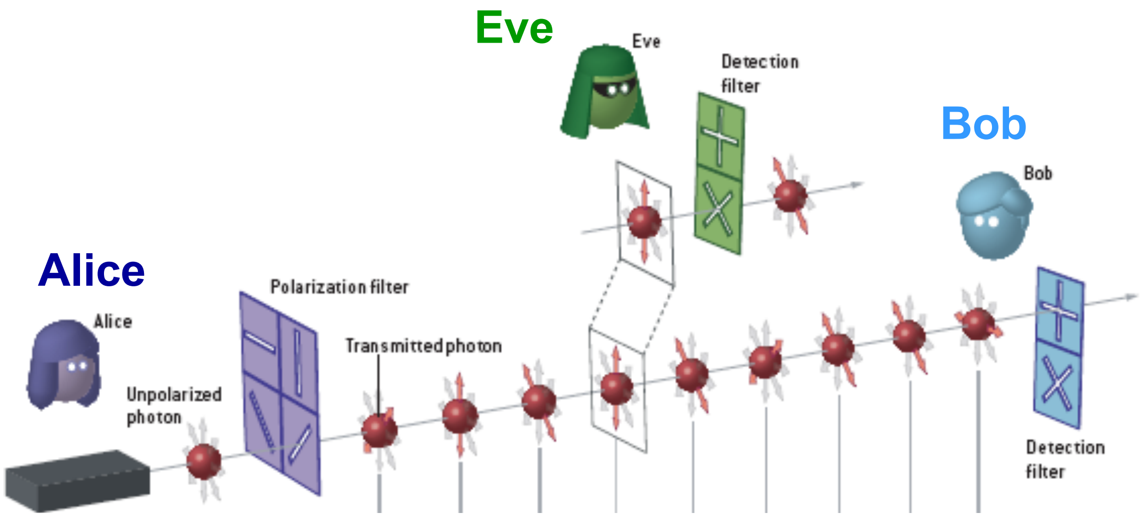

Encryption using quantum properties of single photons

single-photon detector module

Communications in photon-starved environments

free-space optical communications

single-photon GmAPD array

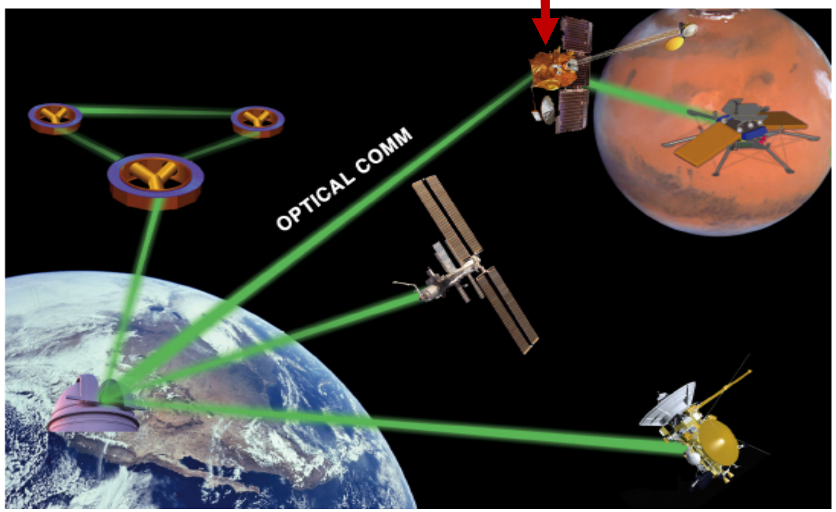

NASA/Jet Propulsion Lab deep-space optical comm

InGaAs(P) APD design for SWIR detection

Two key device regions:

Multiplication region: Create additional carriers by avalanche gain

Absorption region: Absorb photon to create electrical carrier

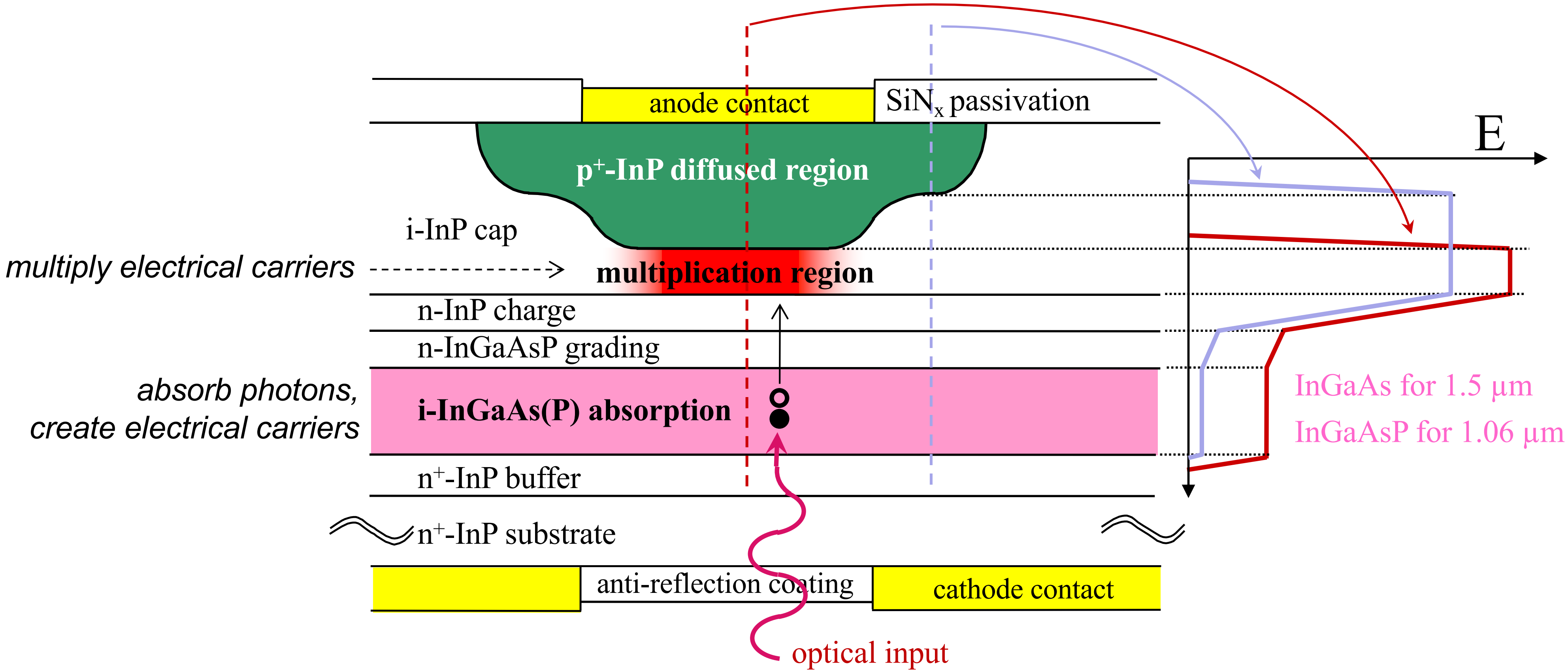

1.5 µm SPAD DCR vs. PDE Performance

Fundamental trade-off: DCR and PDE both increase with bias

State-of-the-art DCR: ~1 kHz at 20% PDE, ~2 kHz at 30% PDE

Higher PDE accessible with larger bias

T = -55°C

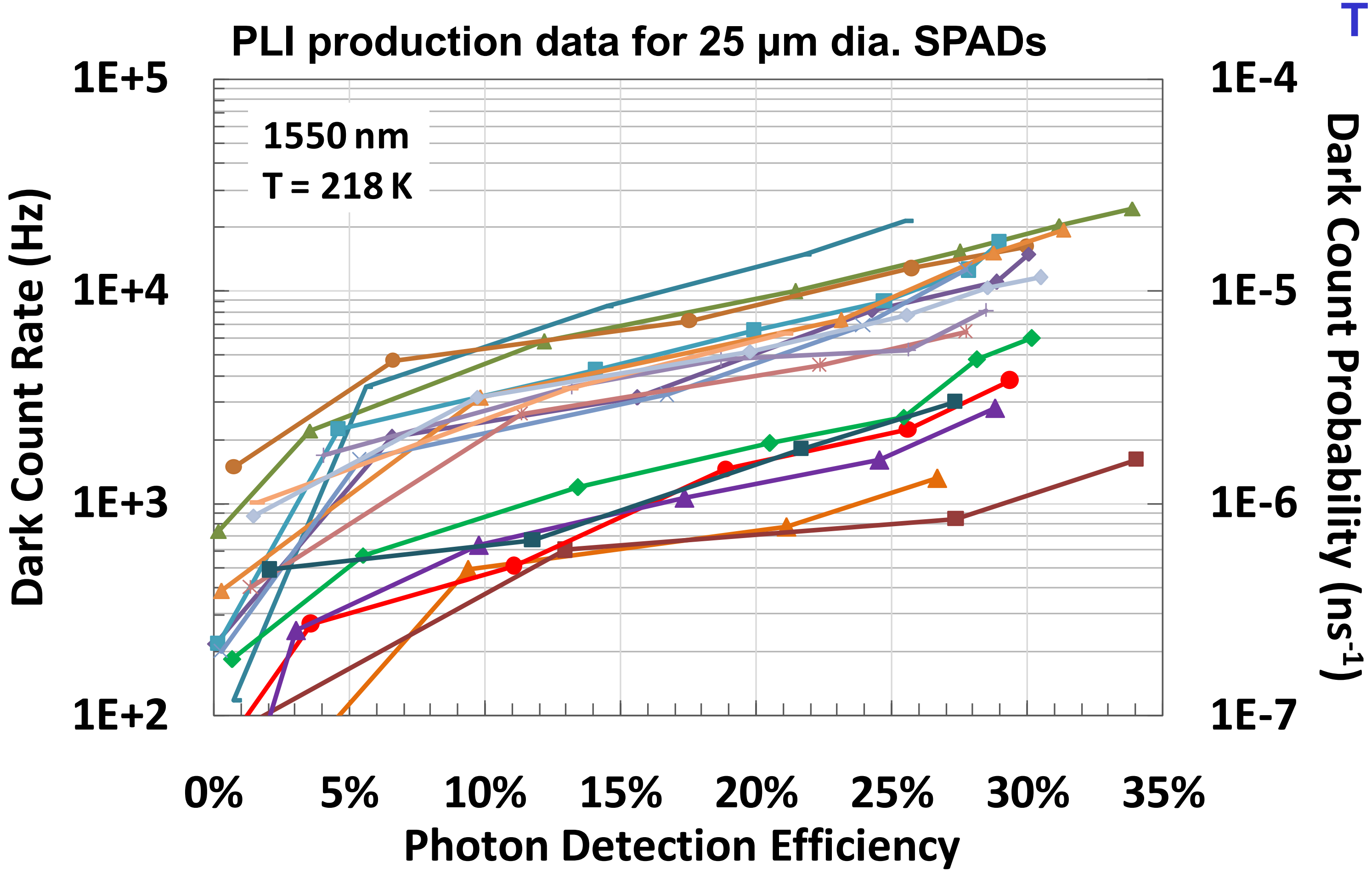

DCR performance distribution

DCR distribution for ~1300 production 1.5 µm GmAPDs at 20% PDE

- ~90% of devices: 1 kHz – 10 kHz
- ~10% of devices > 10 kHz (significant outliers)

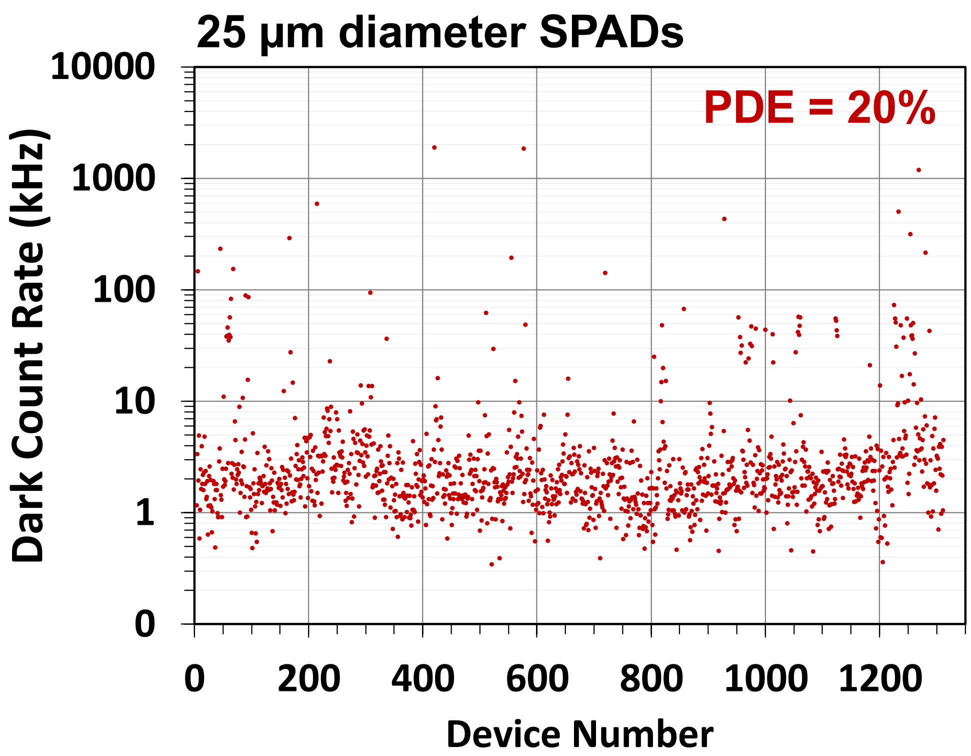

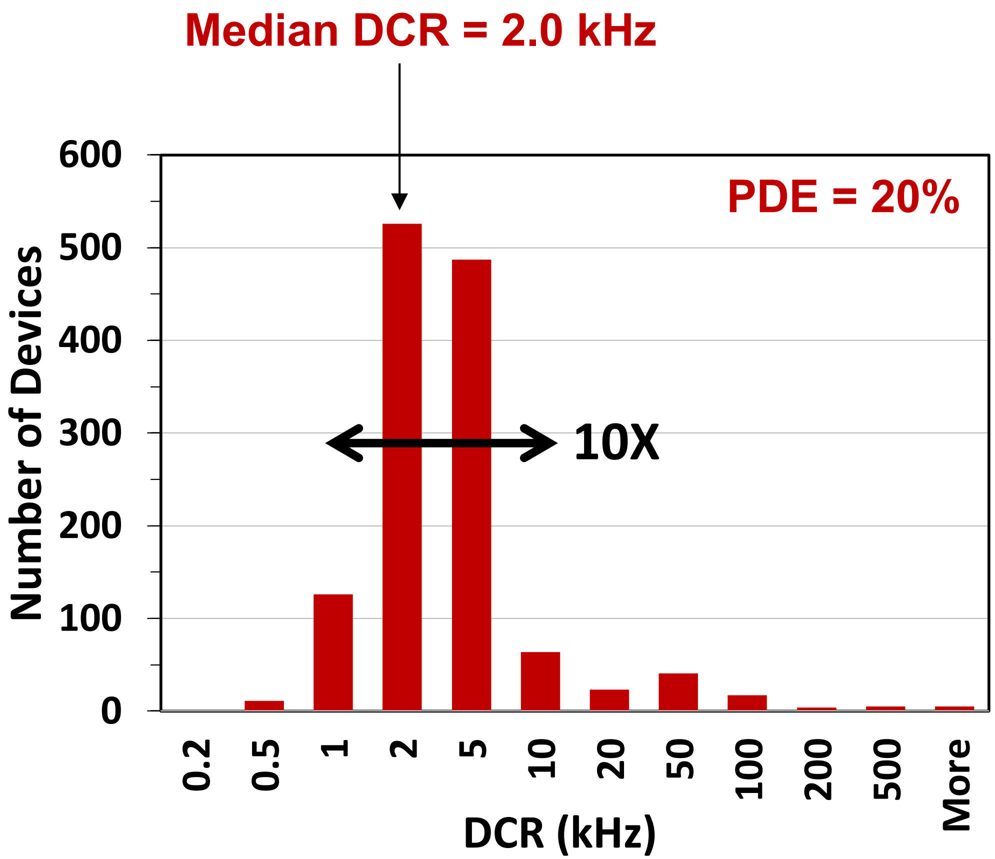

Timing Jitter

Several factors affect GmAPD detection timing

~100 ps jitter for typical operation

Jitter often circuit-limited

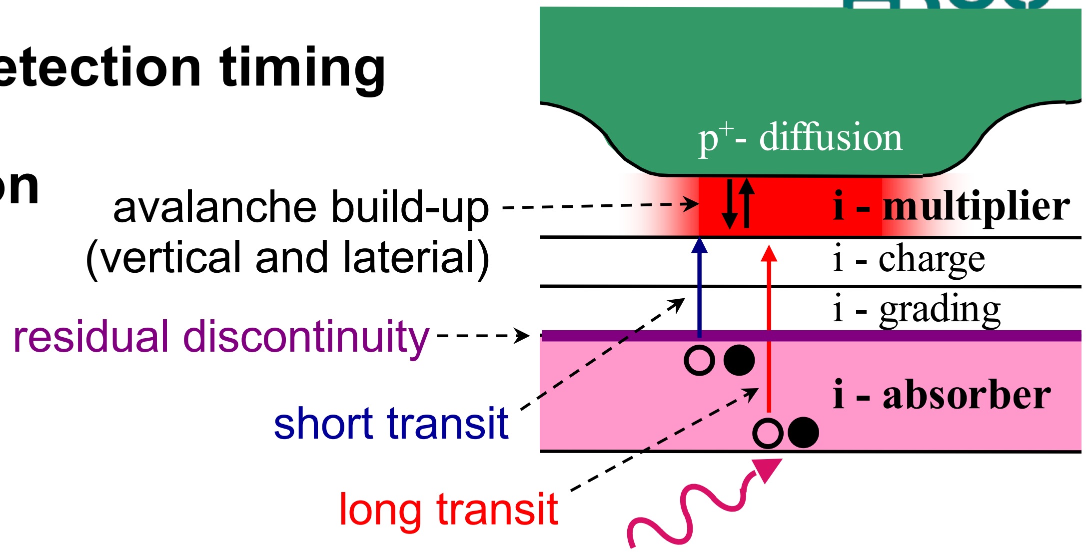

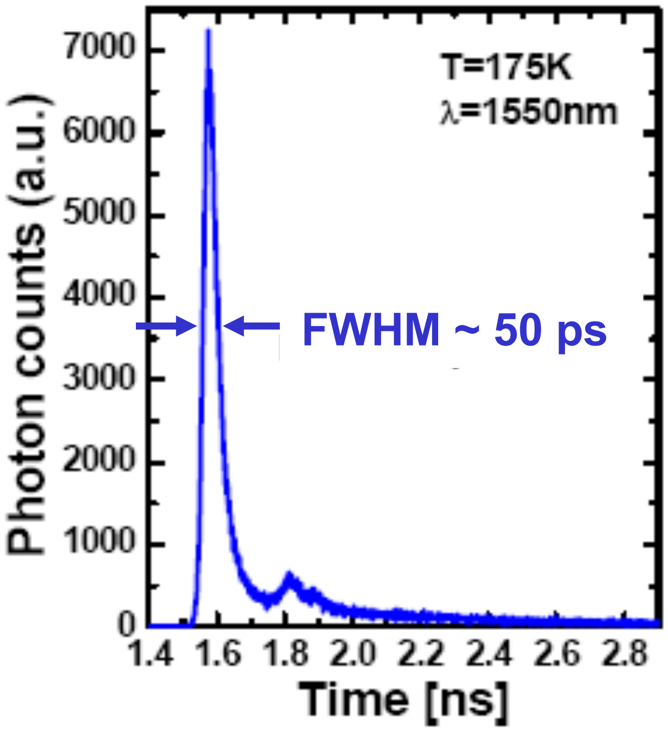

Zappa, Tosi, Cova, SPIE 65830E (2007)

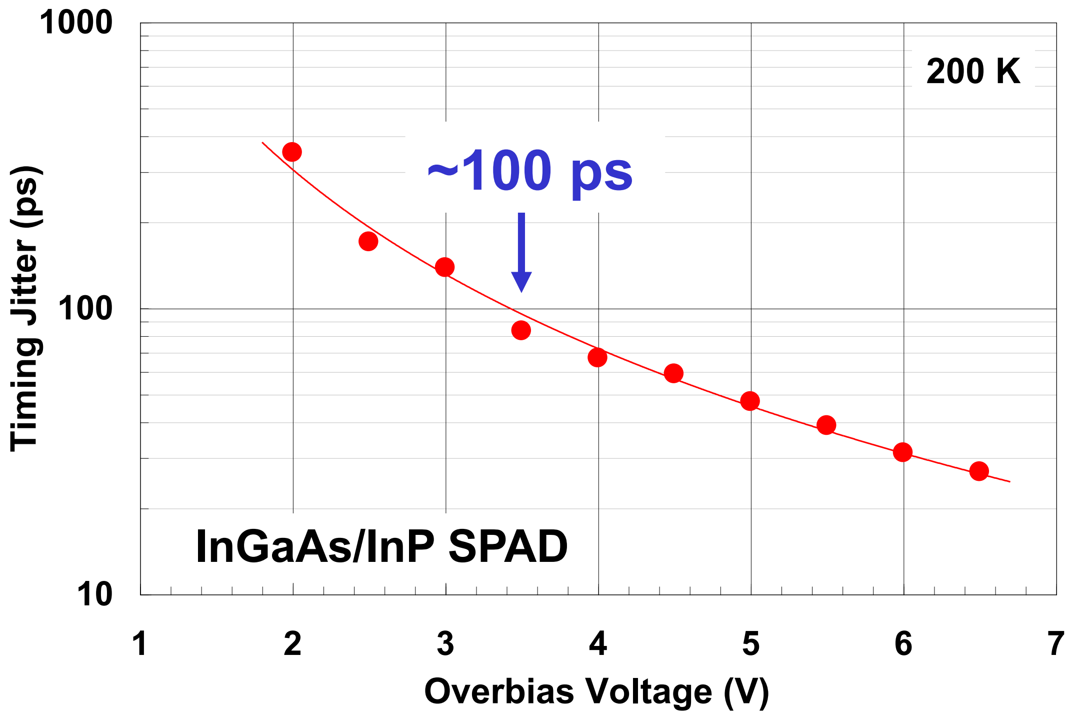

Itzler, et al., J. Modern Opt. 54, 283 (2007)

Afterpulsing and Geiger-mode reset time

Some carriers are trapped during avalanche, then de-trap at later times

Mitigate with longer hold-off (or reset) time…
…but limits APD counting rate

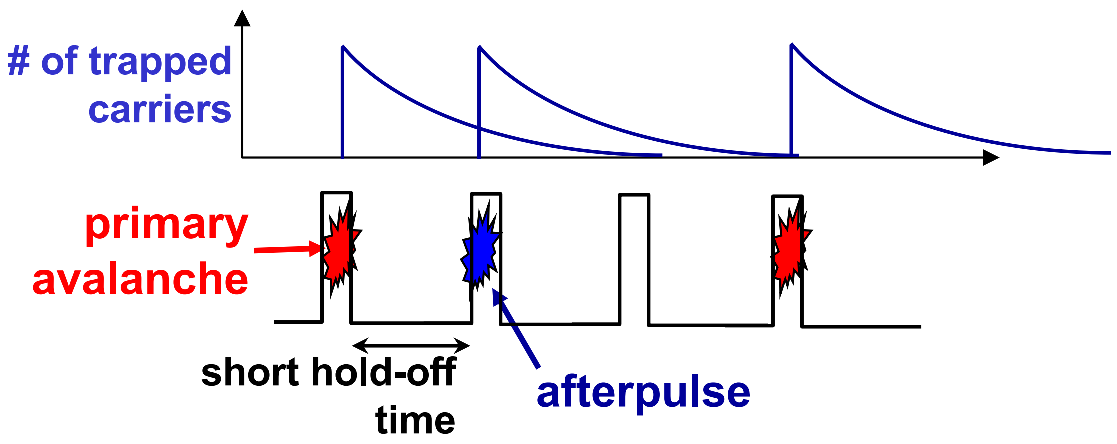

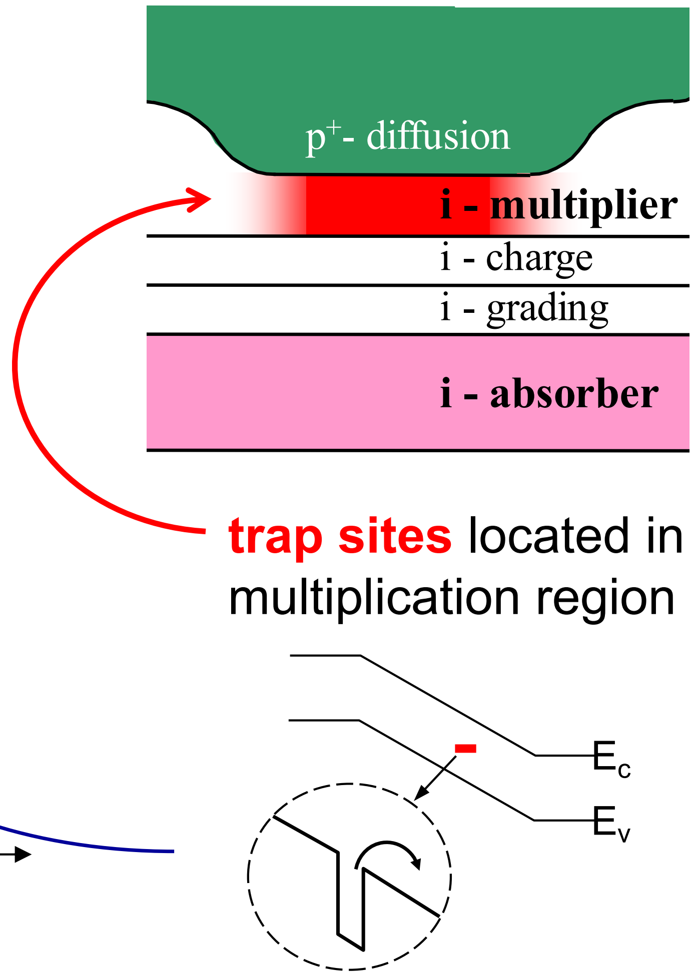

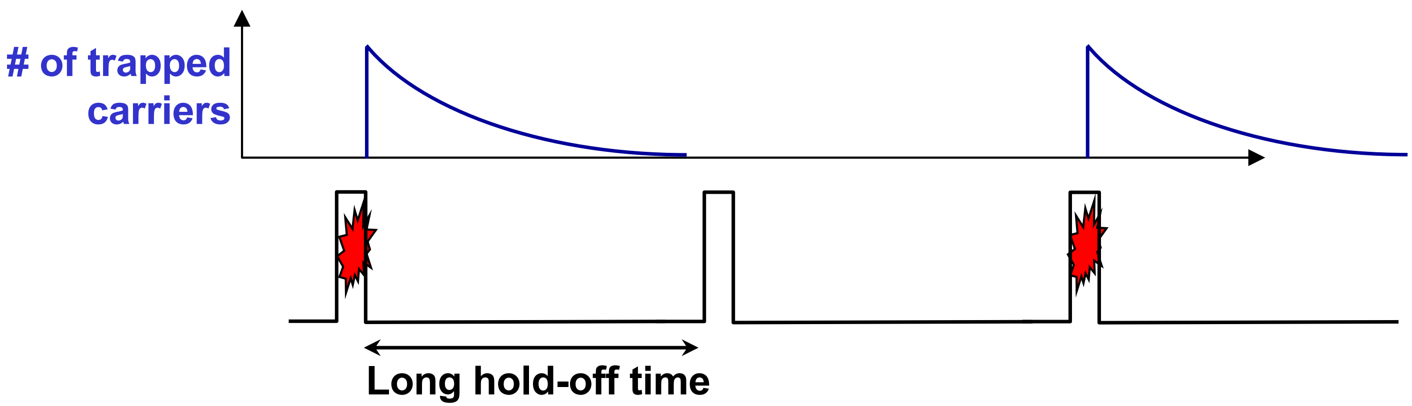

State-of-the-art DCR & PDE (PLI SPADs)

Univ. Geneva (H. Zbinden)

5 Hz DCR at 20% PDE

T = -110°C, 1550 nm

Low temperature

P_{app} ~ 2% (20 μs deadtime)
Free-running (negative feedback APD)

Korzh, et al., APL 104, 081108 (2014)

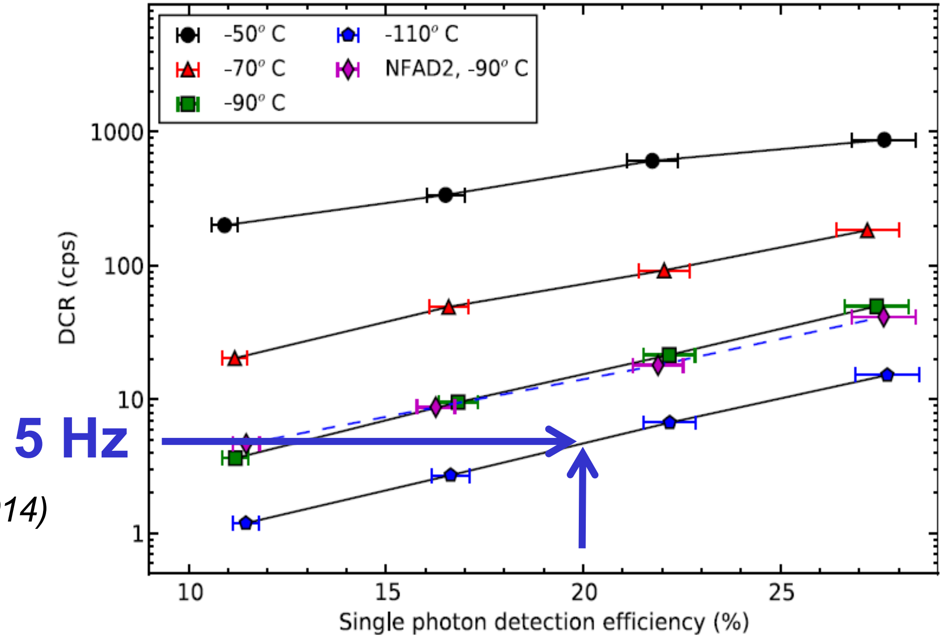

Toshiba / Cambridge, UK

55% PDE (at ~800 kHz)

T = 20°C, 1550 nm

High temperature

P_d ~ 3 x 10^4 per 360 ps gate
P_{app} ~ 15%
~90 ps jitter
Self-differencing with 1 GHz gating
Maximum count rate of 500 MHz

Comandar, et al., JAP 117, 083109 (2015)

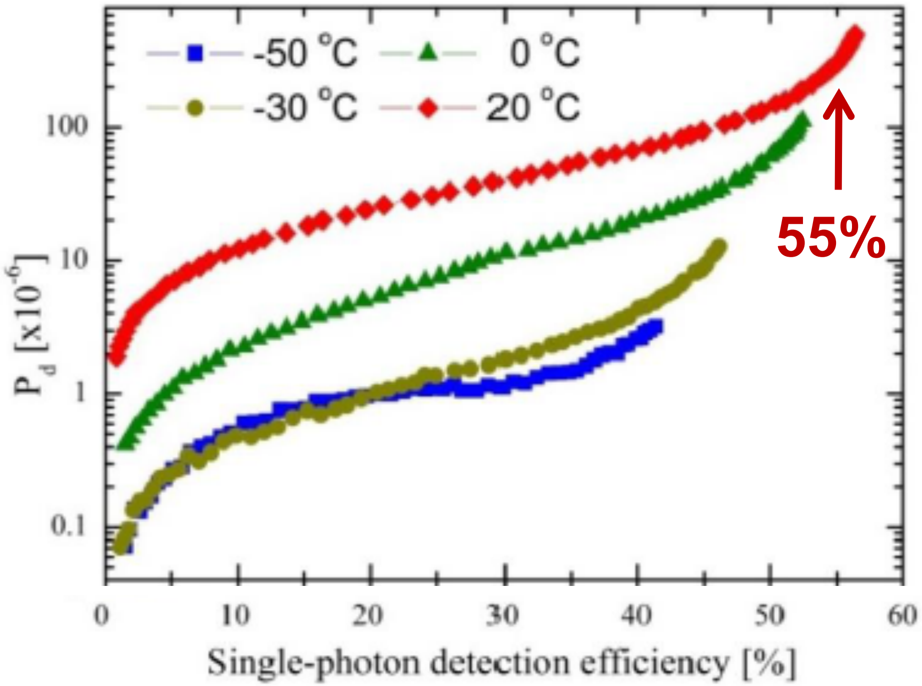

Silicon vs InGaAs/InP SPAD performance

Compare underlying material properties of Si and InGaAs/InP SPADs

Remove role of bandgap → compare at T for which $E_g/2kT$ is equivalent

TOPICAL REVIEW

Advances in InGaAsP-based avalanche diode single photon detectors

Mark A. Itzler[a*], Xudong Jiang[a], Mark Entwistle[a], Krystyna Slomkowski[a], Alberto Tosi[b], Fabio Acerbi[b], Franco Zappa[b] and Sergio Cova[b]

[a]Princeton Lightwave Inc., 2555 US Route 130 S., Cranbury, NJ 08512, USA; [b]Dipartimento di Elettronica e Informazione, Politecnico di Milano, Milan I-20133, Italy

Journal of Modern Optics
Vol. 58, Nos. 3–4, 10–20 February 2011, 174–200

Table 1. Comparison of state-of-the-art performance for Si and InGaAs/InP SPADs.

	Si[a]	InGaAs/InP
Temperature	20°C	−70°C
Active region diameter	50 μm	
Wavelength	400–800 nm	1000–1600 nm
DCR and PDE[b]	10 kHz at 60%	–
	2 kHz at 40%	10 kHz at 40%
	0.5 kHz at 20%	2 kHz at 20%
	–	1 kHz at 10%
Min hold-off for 1% afterpulsing[c]	~10 ns	~100 ns
Jitter (FWHM)	30–50 ps	50–100 ps

[a]Si SPAD performance corresponds to thin Si SPAD structures as in [75]. [b]Si PDE values are cited for 550 nm, for which the highest Si PDE is obtained. [c]Assumes 20% PDE and free-running operation with fast active quenching of a few ns.

Progress on absolute performance in InGaAs/InP using smaller active regions

DCR: ~5X superiority in material properties for Silicon

Afterpulsing: ~10X superiority in material properties for Silicon

Argo AI Proprietary

Outline

Basics of InGaAs/InP SPADs

Device performance attributes

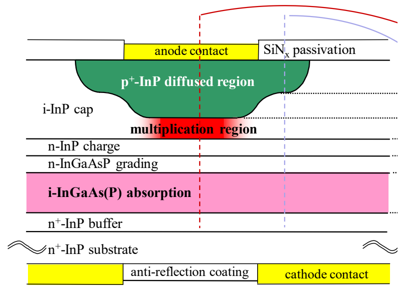

GmAPD cameras for airborne 3D LiDAR imaging

FPA integration and camera performance

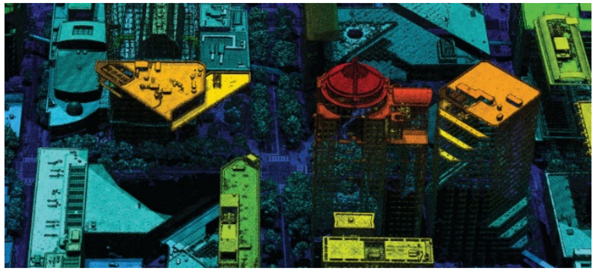

GmAPDs for 3D LiDAR in autonomous vehicles

Design considerations and demonstrator performance

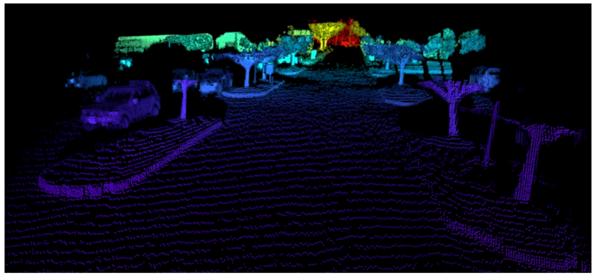

Geiger-mode APD detector array design

APDs scalable to large-format arrays → semiconductor scaling

GmAPD in every pixel

100 μm pixel pitch

GmAPD schematic

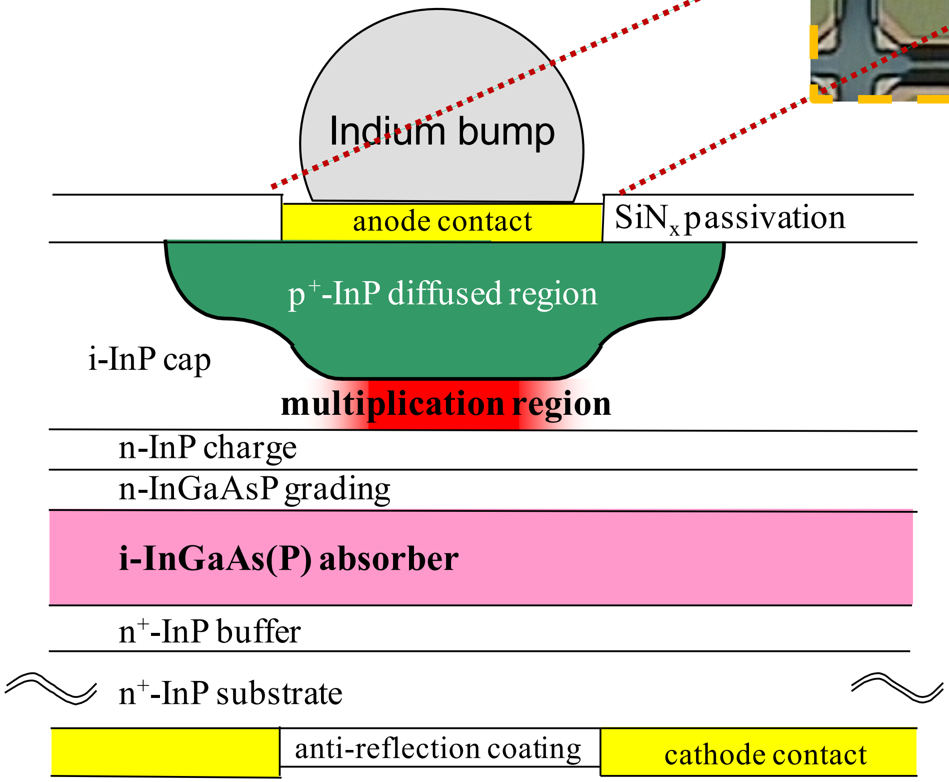

GmAPD pixel

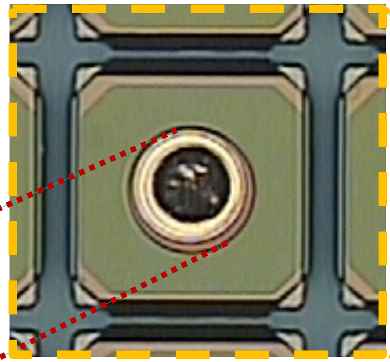

32 x 32 GmAPD array

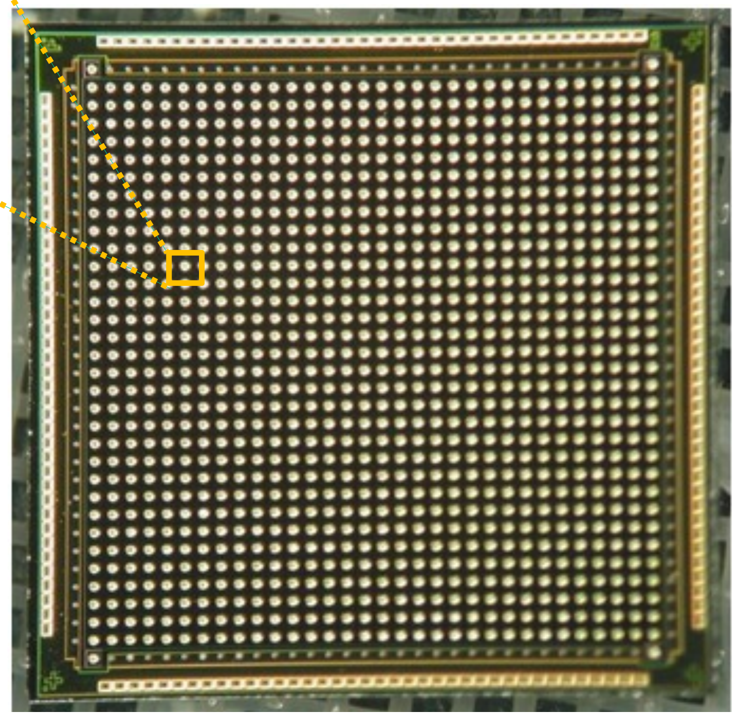

Focal plane array integration: 32 x 32

Focal Plane Array (FPA) integration of three semiconductor chips:

InP Photodiode array (PDA), GaP Microlens array (MLA) and CMOS Readout Integrated Circuit (ROIC)

32 x 32 PDA

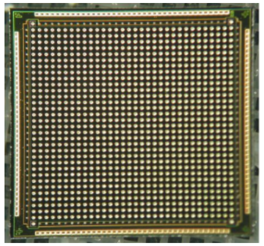

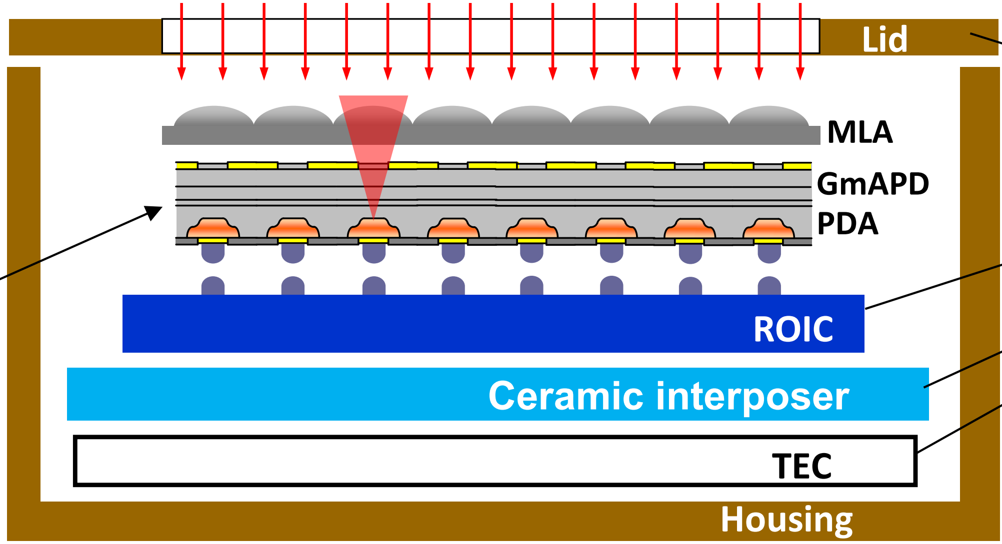

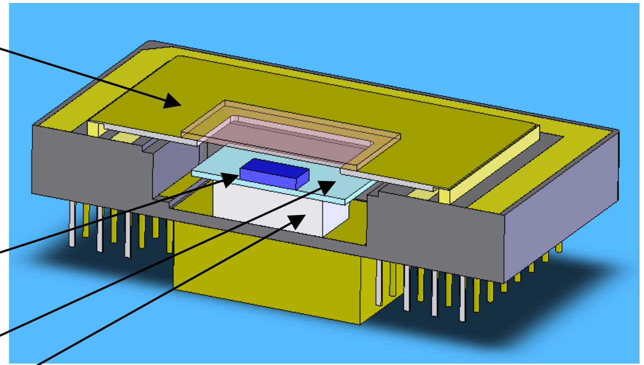

FPA solid body model

100 µm pitch

FPA chip stack on interposer

Microlens array (MLA) on top

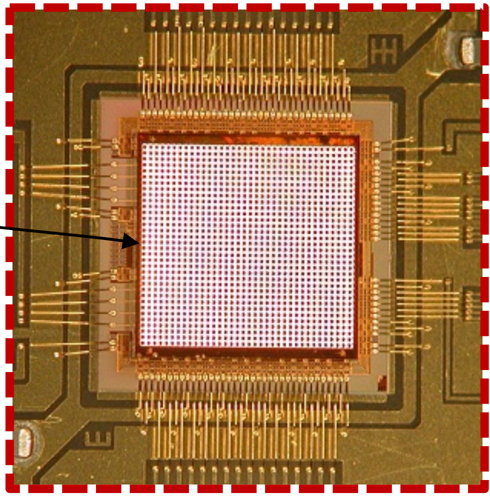

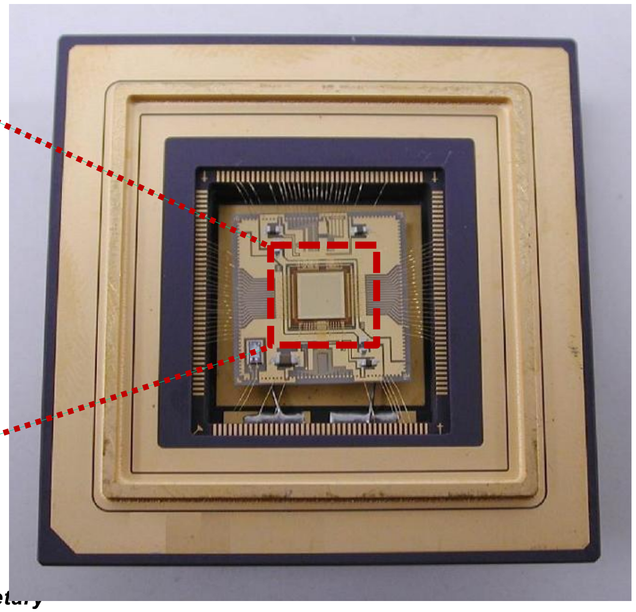

Full FPA assembly without lid

Focal plane array integration: 128 x 32

Same FPA assembly platform for 128 x 32 (50 µm pixel pitch)

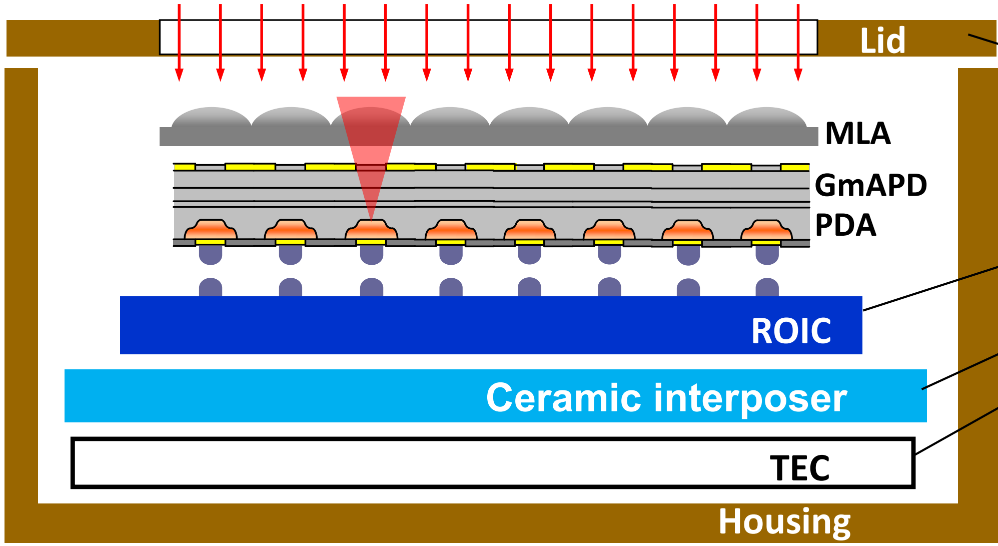

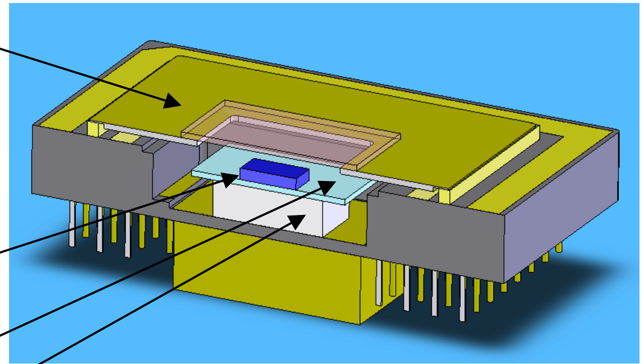

FPA solid body model

50 µm pitch

128x32 FPA chip stack on interposer

Microlens array (MLA) on top

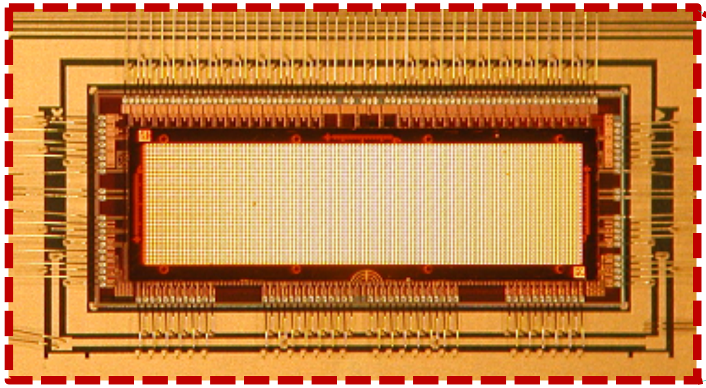

128x32 FPA assembly

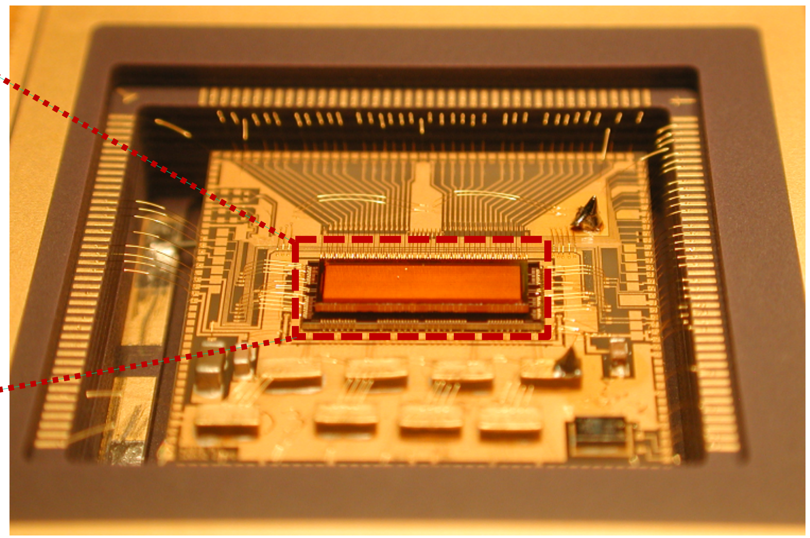

Turn-key camera-level integration

Modular three-board design (FPA, FPGA, I/O)

GUI interface supports all camera functions

10 cm x 10 cm x 9 cm

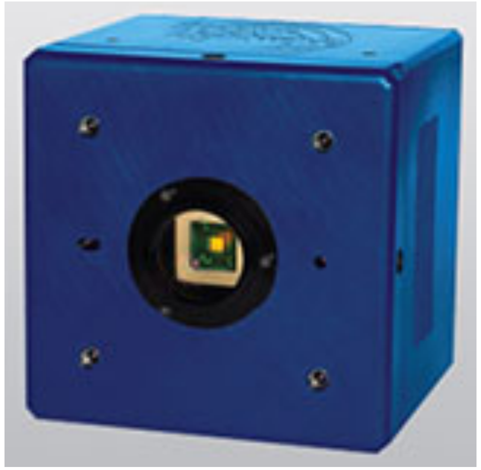

assembled boards

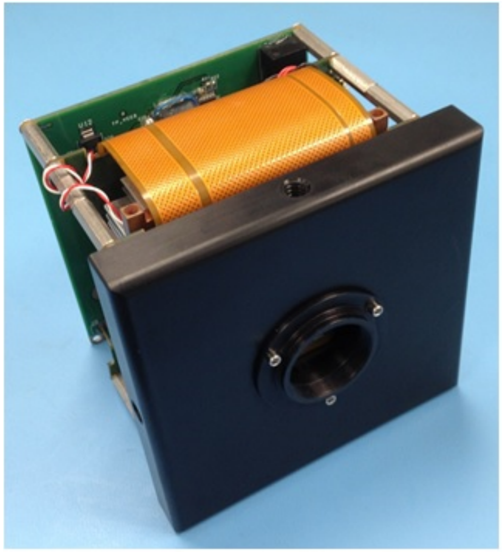

convection cooling

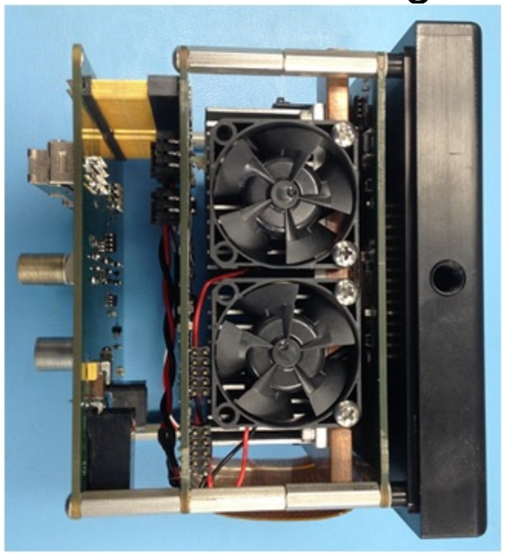

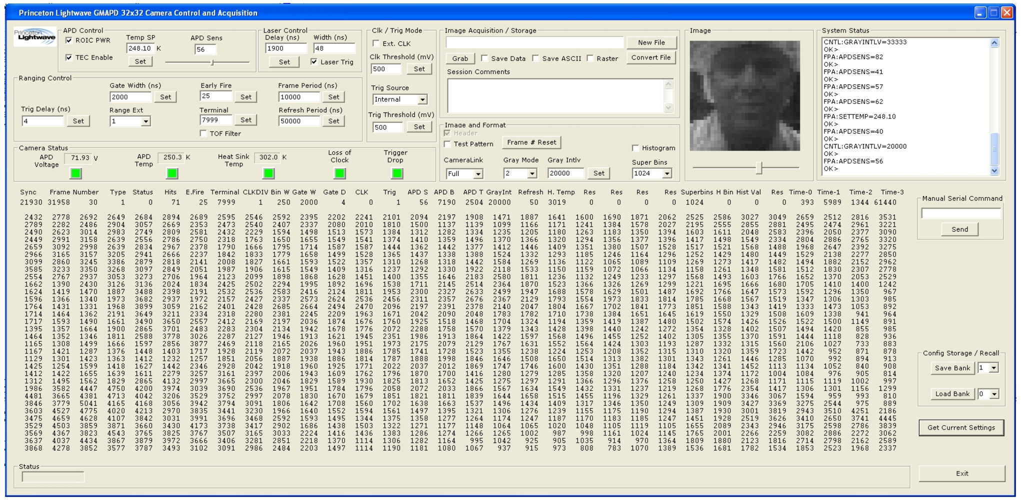

Timing operation for LIDAR imaging

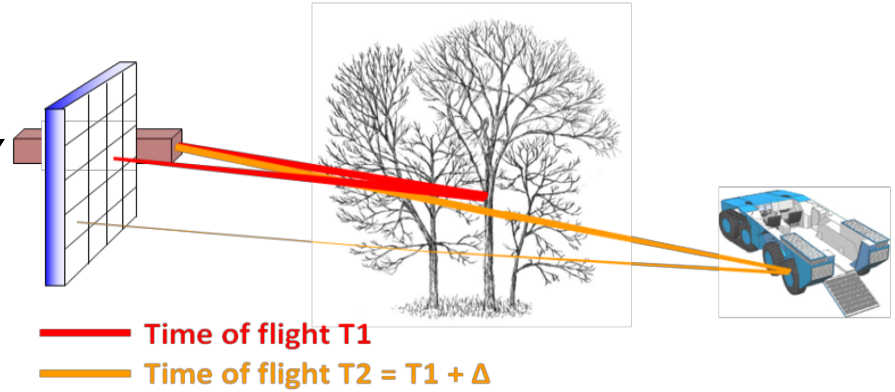

Camera synchronized to pulsed laser

13-bit timing counters in every pixel

0.25 ns time bin resolution (~3 cm)

186,000 frames/sec

Laser launch (e.g., trigger signal from flash detectors)

Counters start

Counters stop

0 – 256 μs

2 μs

8000 bins

3.5 μs

Camera timing: **Programmable delay** | **Range gate** | **Readout**

32 x 32 camera DCR & PDE

Performance maps for all pixels of 1.06 µm detection camera (100% yield)

Dark Count Rate (kHz)

DCR Mean = 2.2 kHz

DC prob. ~ 0.4% / pixel / frame

	1	2	3	4	5	6	7	8	9	10	11	12	13	14	15	16	17	18	19	20	21	22	23	24	25	26	27	28	29	30	31	32
1	2	2	2	2	2	2	2	2	2	2	2	3	2	2	2	2	2	3	2	2	2	3	3	2	2	2	3	3	3	3	3	3
2	2	2	2	2	2	2	2	2	2	2	2	2	2	2	2	2	2	2	2	2	2	3	2	2	2	3	2	3	2	3	3	2
3	2	2	2	2	2	2	2	2	2	2	3	2	2	2	2	2	2	3	2	3	2	3	3	3	2	3	2	3	2	4	3	2
4	2	2	2	2	2	2	2	2	2	3	3	2	2	2	3	2	2	2	2	2	2	2	2	3	2	3	2	3	3	3	3	2
5	2	2	3	2	2	2	2	2	2	2	2	2	2	2	2	3	2	2	3	2	2	2	3	2	3	2	3	3	3	3	3	2
6	2	2	2	3	3	2	2	2	2	3	2	2	2	2	2	2	3	2	2	2	2	3	3	3	2	2	2	3	2	2	2	2
7	1	2	2	2	2	2	2	2	2	2	3	2	2	3	2	3	3	2	2	2	2	2	3	2	2	3	2	3	3	3	3	3
8	2	2	3	2	2	3	2	2	2	3	2	3	2	2	2	3	2	3	3	2	3	3	3	3	3	3	3	3	3	2	3	2
9	2	2	2	2	2	2	3	2	3	3	2	3	3	2	3	3	2	2	3	3	3	3	3	3	2	3	3	3	3	3	3	2
10	2	2	2	3	3	2	2	2	3	2	2	2	3	3	2	3	2	3	3	3	3	3	3	3	2	3	3	3	3	3	3	2
11	2	2	3	2	2	3	2	2	3	3	2	3	3	2	2	2	3	2	3	3	2	3	3	3	3	3	3	2	3	4	2	2
12	2	2	2	3	3	3	2	2	2	2	3	3	2	2	2	3	3	3	2	3	3	2	3	2	3	3	2	3	3	3	3	2
13	1	2	2	3	3	3	2	2	2	2	2	2	2	3	2	3	3	3	3	3	3	3	2	3	3	3	3	3	2	2	2	2
14	2	2	2	2	3	3	2	3	3	2	3	2	2	2	3	3	3	3	3	3	3	3	2	2	2	3	2	2	3	2	3	2
15	2	2	2	2	2	2	2	3	2	3	2	2	3	3	2	3	3	3	3	3	3	2	3	3	2	2	3	2	3	2	2	2
16	2	2	2	2	2	2	2	3	2	2	2	2	3	3	2	3	3	3	3	3	3	3	2	2	3	3	2	2	2	2	2	2
17	2	2	2	3	2	2	3	2	2	2	2	3	3	2	3	3	2	2	3	3	2	2	3	3	3	2	2	3	2	2	2	2
18	2	2	2	2	2	2	2	3	2	2	2	2	2	3	3	3	2	2	2	3	3	2	3	3	3	2	2	2	2	2	2	2
19	2	2	2	2	2	2	2	2	2	2	2	3	2	3	3	3	3	3	2	2	3	2	3	2	2	2	3	2	2	2	2	2
20	2	2	2	2	2	2	2	2	2	2	2	2	3	2	3	3	3	3	3	3	3	2	3	2	2	2	2	2	2	2	2	2
21	2	2	2	2	2	2	2	2	2	3	2	2	3	2	2	3	3	2	3	2	2	3	2	2	3	2	2	2	2	2	2	2
22	2	2	2	3	2	2	2	2	3	4	3	2	3	2	3	2	3	2	2	2	2	2	3	3	2	2	2	2	2	2	2	2
23	2	2	2	2	2	3	2	2	2	2	2	2	2	2	2	2	2	2	2	2	2	2	2	2	3	2	2	2	2	2	2	1
24	2	2	2	2	2	2	2	2	2	2	2	2	2	2	3	2	2	2	2	2	2	2	2	3	2	2	2	2	2	2	2	2
25	2	2	2	2	2	2	2	2	3	2	2	2	2	2	2	2	2	2	2	2	2	2	2	2	2	2	2	2	2	2	1	2
26	2	2	2	2	2	2	2	2	2	2	3	2	2	2	2	2	2	2	2	2	2	2	2	2	2	2	2	2	2	2	2	1
27	2	2	2	2	2	3	2	2	2	2	2	2	2	2	2	2	2	2	2	2	2	2	2	2	2	2	2	2	2	1	2	1
28	2	2	2	2	2	2	3	2	2	2	2	2	2	2	2	2	2	2	2	2	2	2	2	2	2	2	2	2	2	2	2	1
29	2	2	2	2	2	2	2	2	2	2	2	2	2	2	3	2	2	2	2	2	2	2	2	2	2	2	2	2	2	1	2	1
30	2	2	2	2	2	2	2	2	2	2	2	2	2	2	2	2	2	2	2	2	2	2	2	2	2	2	2	2	1	2	1	1
31	2	2	2	2	2	2	2	2	2	2	2	2	2	2	2	1	2	2	2	2	2	1	1	2	2	2	1	1	1	1	1	1
32	2	2	1	1	1	1	2	2	2	2	2	1	1	2	2	2	2	1	1	2	2	2	1	1	1	1	1	1	1	1	1	1

2.2 kHz mean @ 30% PDE

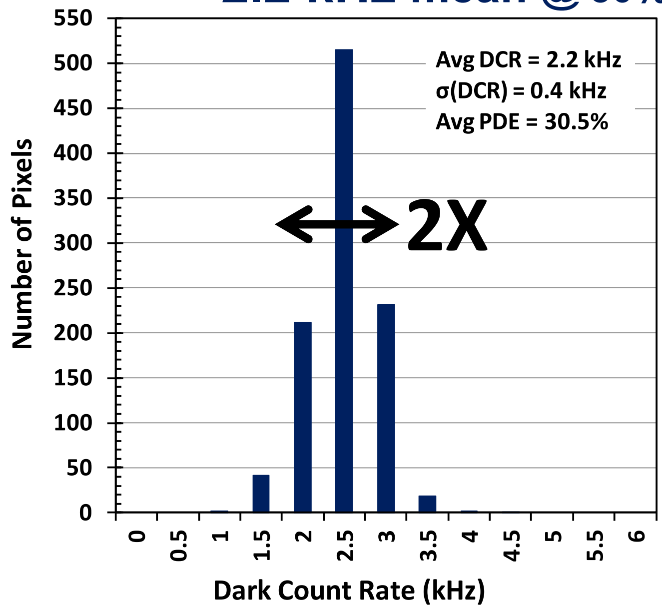

-25°C

Photon Detection Efficiency (%)

PDE Mean = 30.5%

	1	2	3	4	5	6	7	8	9	10	11	12	13	14	15	16	17	18	19	20	21	22	23	24	25	26	27	28	29	30	31	32
1	27	30	34	29	29	29	32	28	30	31	31	29	30	33	31	31	32	32	33	35	32	35	32	37	35	35	34	32	30	30	32	28
2	28	31	30	32	26	26	30	31	31	31	29	29	34	31	36	34	33	34	34	34	29	31	33	31	34	32	32	31	37	30	31	28
3	28	25	32	31	28	30	32	31	30	30	30	32	33	32	32	31	34	33	35	31	31	33	32	32	34	35	32	32	32	34	33	28
4	25	25	32	32	30	29	29	32	29	30	33	31	32	33	34	36	33	36	32	36	38	36	36	32	34	31	32	32	31	32	33	29
5	28	25	28	30	31	34	32	29	26	29	32	35	35	36	32	34	34	34	34	35	35	36	35	36	34	34	34	31	30	29	31	26
6	26	27	31	30	28	33	29	32	29	35	35	34	36	33	31	35	36	35	34	36	38	35	37	36	37	33	32	31	34	32	36	29
7	26	29	32	28	31	35	34	30	33	35	31	33	37	35	33	33	35	37	33	32	33	33	35	36	34	33	34	35	30	31	31	31
8	28	31	29	31	32	28	31	30	33	32	33	34	35	37	34	37	35	34	36	36	34	35	37	36	38	37	36	34	33	31	34	30
9	29	23	30	34	36	29	29	31	32	32	35	34	38	35	33	32	34	36	36	39	36	37	36	39	38	37	36	33	31	36	34	31
10	28	25	35	35	29	32	32	33	33	35	36	32	36	37	37	34	35	33	34	33	34	36	35	33	36	37	32	37	34	33	34	29
11	23	26	29	31	31	33	31	36	33	35	34	32	35	36	35	37	35	36	36	34	34	35	35	36	34	30	36	31	40	41	33	28
12	26	24	31	33	30	32	34	29	32	32	33	36	37	36	38	34	33	35	34	39	34	34	36	33	34	31	32	36	34	37	33	27
13	25	28	31	29	34	32	36	31	34	35	34	34	36	38	38	36	35	34	34	33	33	36	36	31	34	33	34	31	32	31	37	31
14	25	30	35	36	33	32	32	35	32	34	33	35	37	37	35	37	37	34	35	33	36	33	34	33	34	31	33	31	31	36	35	29
15	26	28	32	31	32	30	32	34	32	30	35	33	35	34	38	34	37	33	33	38	32	37	32	32	32	33	34	31	31	34	29	30
16	27	30	30	31	32	33	32	31	32	32	32	34	33	33	36	36	37	35	37	34	34	34	32	33	34	34	31	34	35	30	30	31
17	24	27	29	32	28	30	32	34	31	32	32	30	34	34	34	36	35	36	33	36	33	31	31	30	29	31	31	34	32	26	29	25
18	26	25	29	32	30	33	34	34	30	33	31	32	32	33	34	39	37	32	34	31	32	30	34	30	32	36	33	35	28	31	29	28
19	26	27	26	28	31	31	33	32	33	34	30	31	33	34	35	33	32	33	35	36	30	28	32	28	32	34	35	31	30	30	30	28
20	29	26	31	28	28	33	30	33	32	30	26	33	28	34	35	37	29	33	31	33	30	30	29	32	31	33	30	32	32	30	30	27
21	26	27	28	27	27	26	30	31	37	38	29	31	27	32	35	30	35	33	34	34	30	30	30	28	31	27	32	30	30	30	30	32
22	29	28	26	26	29	29	31	31	36	36	32	29	26	33	31	34	33	32	32	28	30	31	33	32	28	32	31	34	31	28	32	27
23	29	28	29	26	24	25	27	27	29	29	31	33	29	30	30	32	33	34	32	32	34	32	33	29	28	29	31	29	27	28	28	30
24	30	26	28	27	25	27	31	27	29	31	32	31	28	30	29	30	32	32	32	32	32	32	30	31	30	30	31	30	30	28	26	25
25	28	27	27	23	27	26	28	31	31	30	31	28	31	29	25	28	31	32	32	28	29	27	30	32	29	32	30	25	31	27	25	25
26	25	28	27	26	25	28	25	28	28	31	28	31	30	27	29	26	26	29	31	31	28	30	28	29	29	30	29	29	26	25	28	24
27	23	26	25	27	27	23	26	26	27	32	30	26	32	26	28	25	26	25	27	28	28	29	28	28	28	25	28	26	25	27	27	22
28	23	26	28	25	26	26	23	25	28	28	29	28	28	27	25	26	27	26	25	25	24	29	31	27	28	28	23	25	26	26	23	23
29	23	24	25	26	25	26	26	28	26	27	28	29	27	25	26	28	27	29	27	24	26	28	26	27	27	25	27	25	28	25	25	23
30	22	24	24	26	24	25	24	23	27	27	29	26	26	28	28	25	25	29	26	24	26	28	26	30	24	21	22	24	24	24	24	21
31	20	21	24	23	23	22	22	24	23	25	26	26	26	24	23	25	22	28	26	21	24	25	28	24	22	24	24	24	23	22	22	19
32	21	24	23	20	23	20	22	24	20	22	22	26	24	23	21	22	24	26	21	21	26	26	27	26	28	22	20	22	25	20	22	23

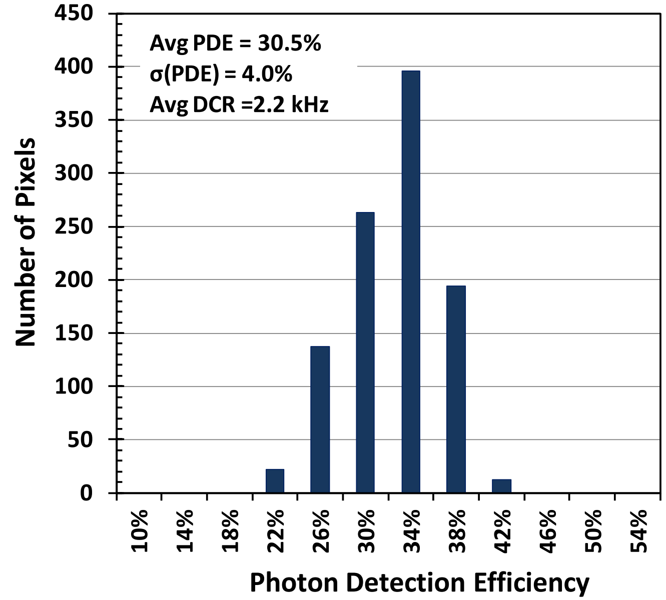

FPA DCR contrasted with discrete SPADs

FPA distribution over ~1000 pixels much more uniform

Array singulation
Flip-chip bonding
Indium bumps

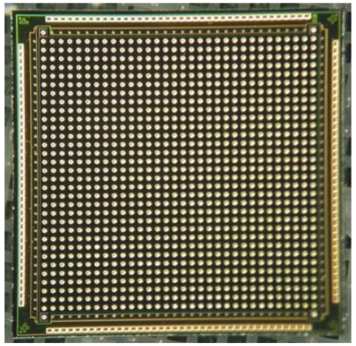

4 mm

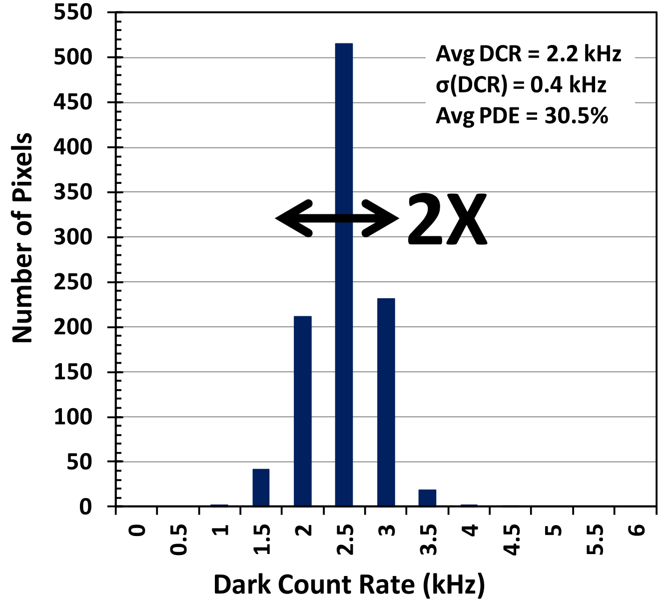

-25°C

Discrete device singulation
Die pick & place
Die bonding to carrier
Wire bonding

0.4 mm

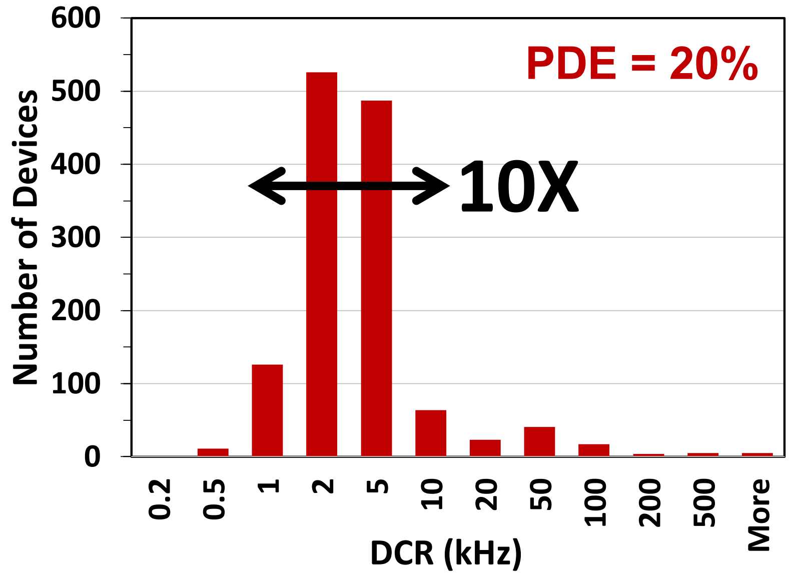

Implies DCR degradation due to additional back-end assembly & packaging processes

GmAPDs with reduced size detectors

Performance enhancements using reduced active areas

DCR, afterpulsing, crosstalk, radiation tolerance

Primary trade-off: optical coupling and assembly

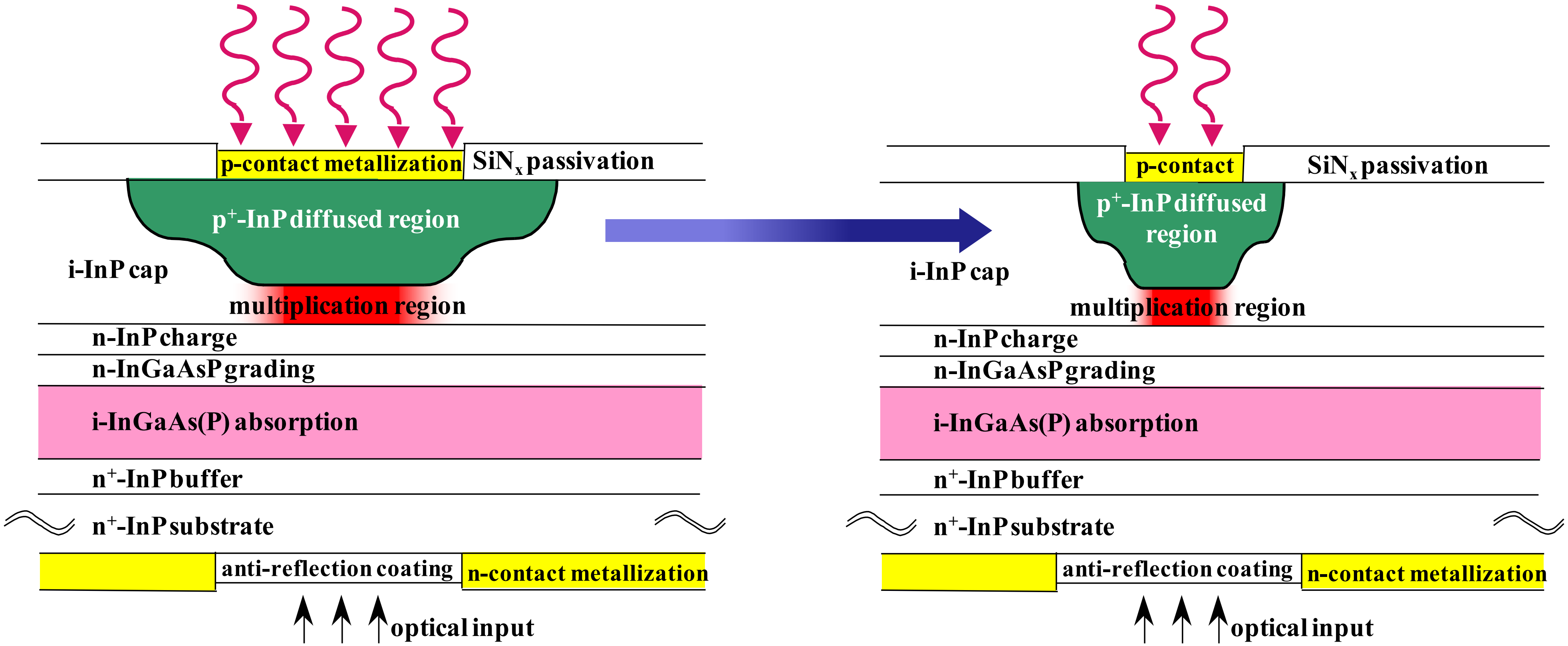

Scaling of FPA format for 128x32 camera

128 x 32 camera with 50 µm pitch, improved PDE vs. DCR

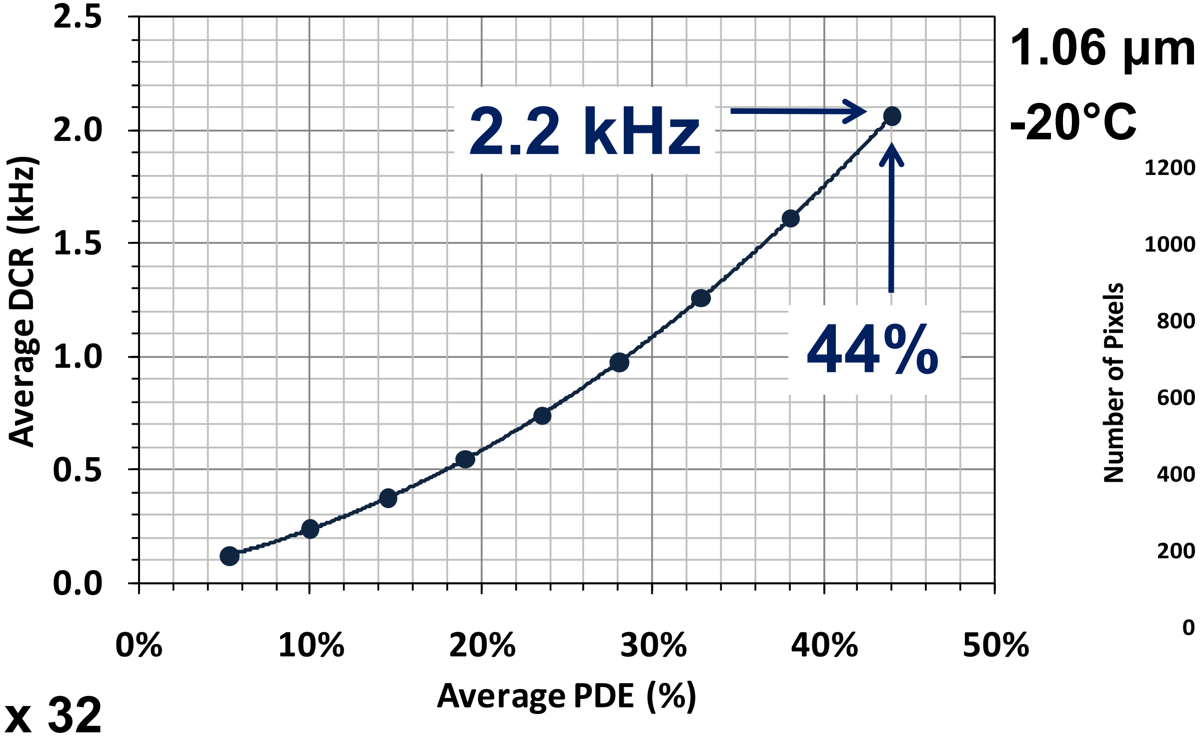

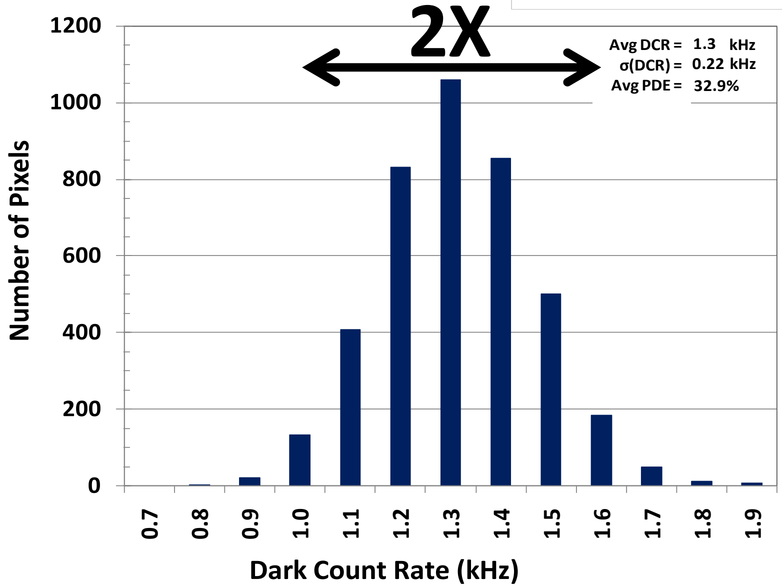

128 x 32

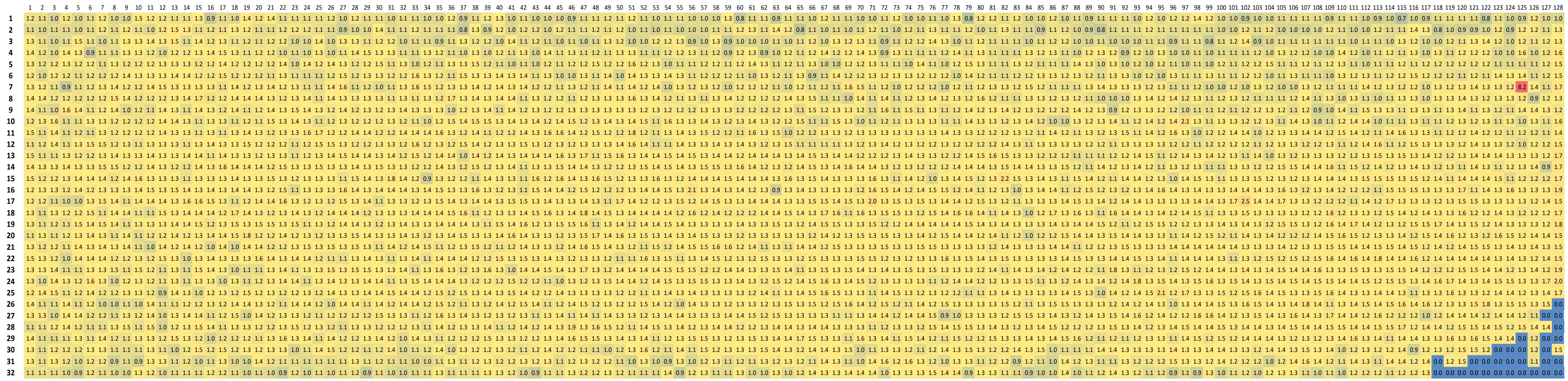

Arrays of GmAPDs have optical crosstalk

Single photons emitted during avalanche can trigger neighboring pixels

- Spatial correlation roughly $1/R^2$
- Spatial patterning from backside reflections
- Temporal correlation on ns-scale
- Various strategies to mitigate crosstalk

21 x 21 spatial map of crosstalk probability

4	0	0	0	5	0	0	2	1	1	4	3	1	2	0	2	2	1	1	1	1
2	2	5	3	2	0	1	4	1	0	2	1	2	3	0	0	0	1	0	1	1
0	3	2	1	2	1	6	5	8	4	6	7	3	3	4	2	2	2	1	0	1
2	6	1	3	1	3	3	3	3	5	9	4	4	1	3	3	3	0	3	1	3
0	2	2	4	5	3	4	0	13	2	11	6	13	3	2	4	4	3	1	2	3
0	2	1	3	4	2	6	3	10	4	10	5	3	7	9	5	2	3	4	4	1
3	1	3	4	8	6	7	12	20	16	25	9	23	16	12	3	5	4	3	1	4
1	3	7	3	5	8	7	11	13	15	17	17	13	18	6	9	3	3	3	2	0
6	3	2	4	12	8	22	17	69	31	90	37	61	16	31	5	17	2	5	3	3
2	3	1	6	5	6	9	14	27	72	37	69	33	14	12	6	4	1	5	2	1
4	2	6	8	16	13	30	20	97	226		201	92	18	36	11	11	4	2	5	7
1	2	2	3	7	6	11	17	50	84	58	83	44	12	14	6	5	2	0	1	4
0	2	3	5	26	9	23	16	75	41	81	36	62	11	21	6	10	2	2	2	7
2	0	5	5	3	5	6	14	10	10	19	20	10	17	4	2	7	5	5	1	1
0	0	3	9	9	8	13	11	19	20	41	14	32	9	11	5	6	2	4	2	1
1	0	2	5	3	1	4	2	4	3	3	8	10	3	2	2	3	7	2	2	1
1	3	3	4	4	2	10	8	6	4	10	5	7	5	10	3	4	3	3	4	5
1	1	0	0	2	2	3	2	0	5	3	2	4	5	1	2	2	1	3	4	2
0	5	7	2	7	2	1	3	4	6	3	8	4	4	2	4	2	1	4	2	1
1	0	0	2	1	0	3	1	2	1	3	5	2	1	1	3	1	0	1	2	1
1	1	0	0	5	2	1	4	1	2	3	2	1	2	2	1	1	3	0	0	2

Structure in spatial map

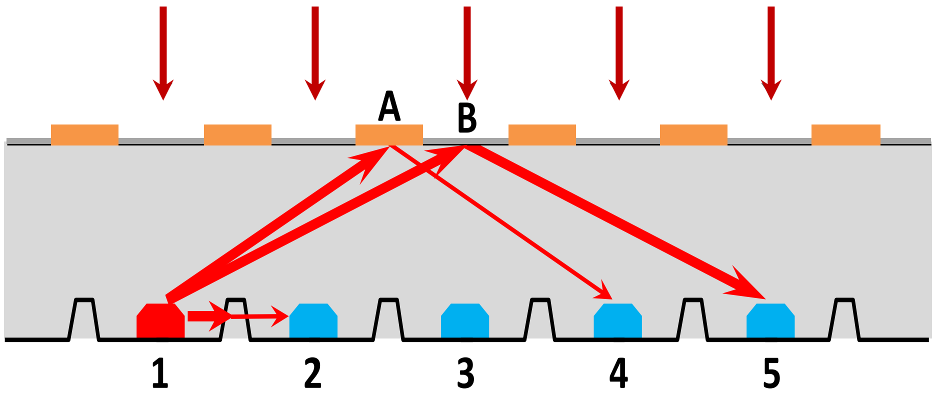

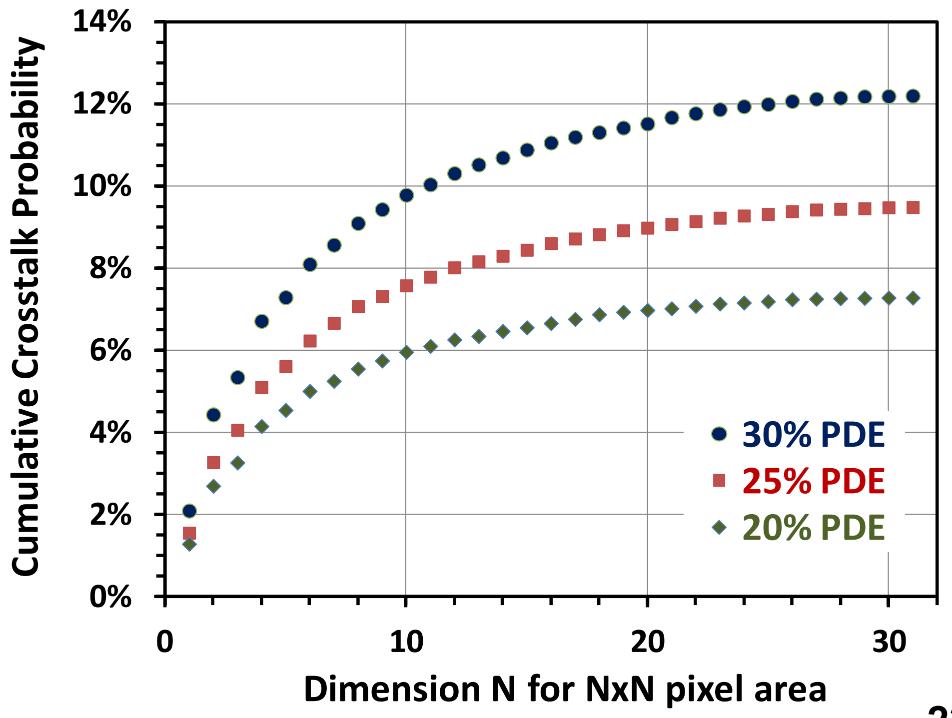

Geiger-mode 3D LiDAR mapping

GmAPD-based commercial mapping systems by Harris Corp.

based on PLI 128 x 32 GmAPD cameras

enables 10X faster data collection than other LIDAR technologies

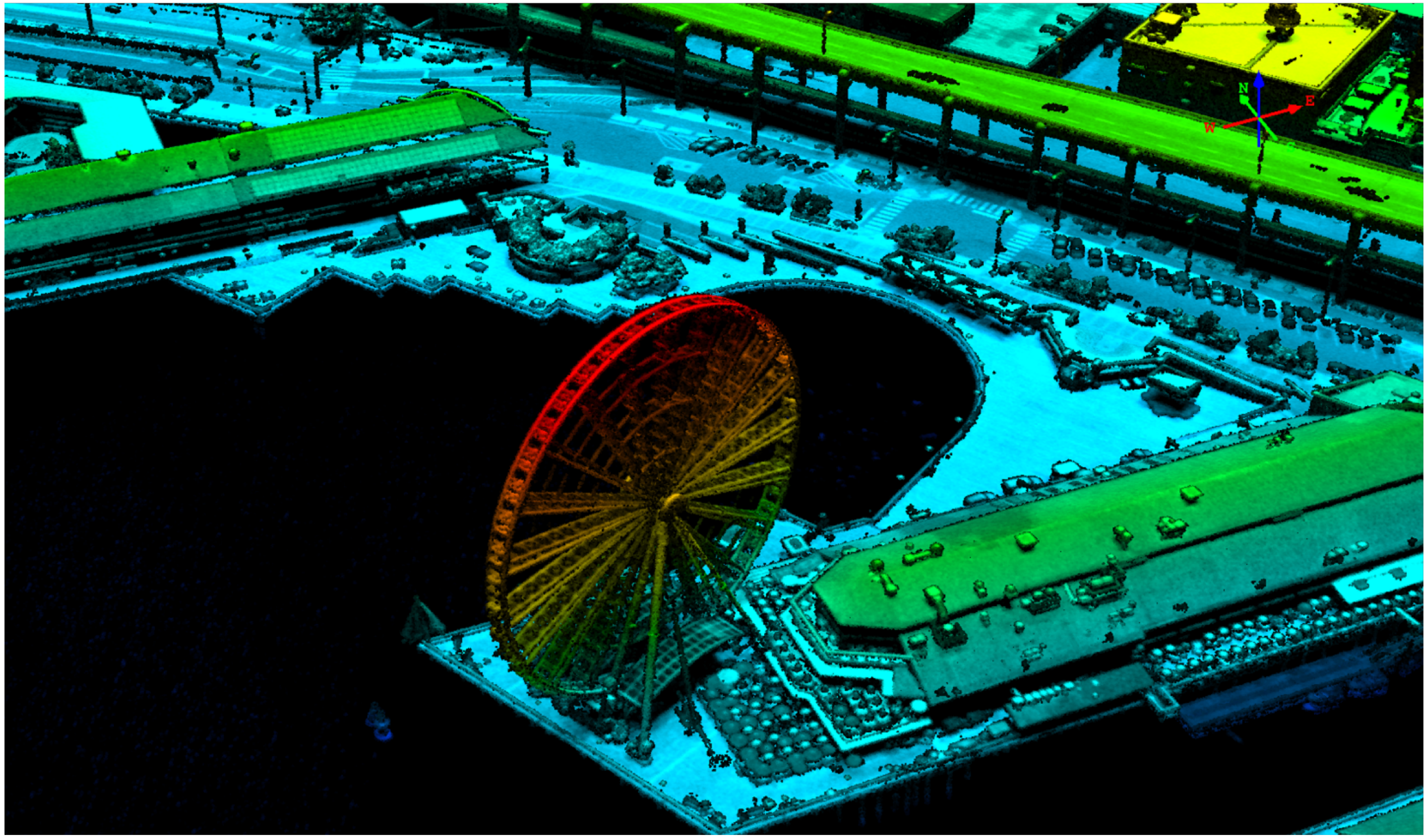

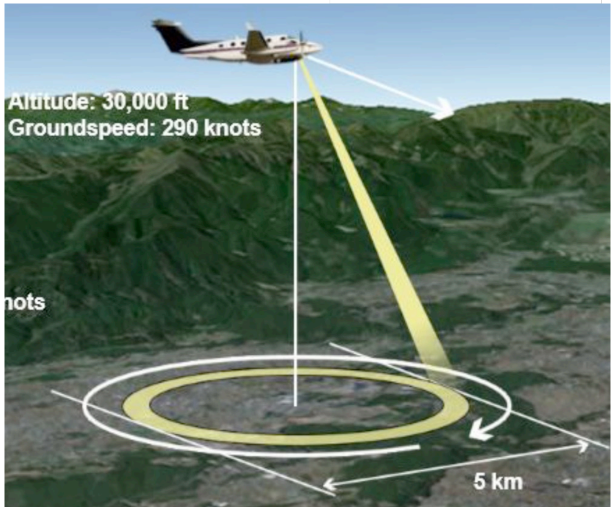

aerial photo: Seattle ferris wheel

imagery courtesy of HARRIS

Airborne navigation and target ID

LiDAR for autonomous helicopter navigation for Sikorsky Black Hawks

- United Technologies Aerospace Systems LiDAR based on PLI GmAPD cameras
- Key self-flying demonstration in Oct 2015
- Retrofit up to 2500 Blackhawks

LiDAR for object identification in targeting pods

- Customized camera formats for defense prime contractors
- Successful flight tests demonstrating technology capability

Outline

Basics of InGaAs/InP SPADs

Device performance attributes

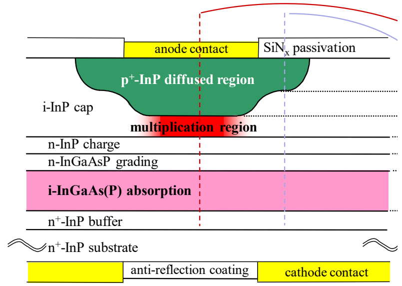

GmAPD cameras for airborne 3D LiDAR imaging

FPA integration and camera performance

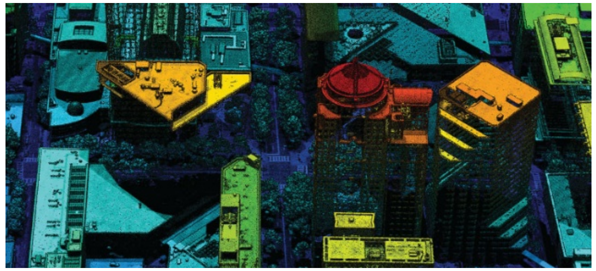

GmAPDs for 3D LiDAR in autonomous vehicles

Design considerations and demonstrator performance

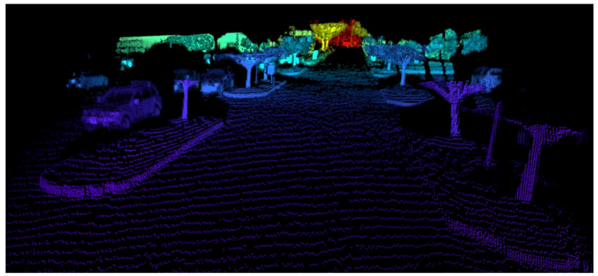

Geiger-mode LiDAR for shorter range?

Autonomous vehicles: most exciting short-range LiDAR application

Market size, societal impact

Safety imperative for sensors with complementary modalities

Wide consensus that driverless car sensor suite will have:

LiDAR Cameras RADAR

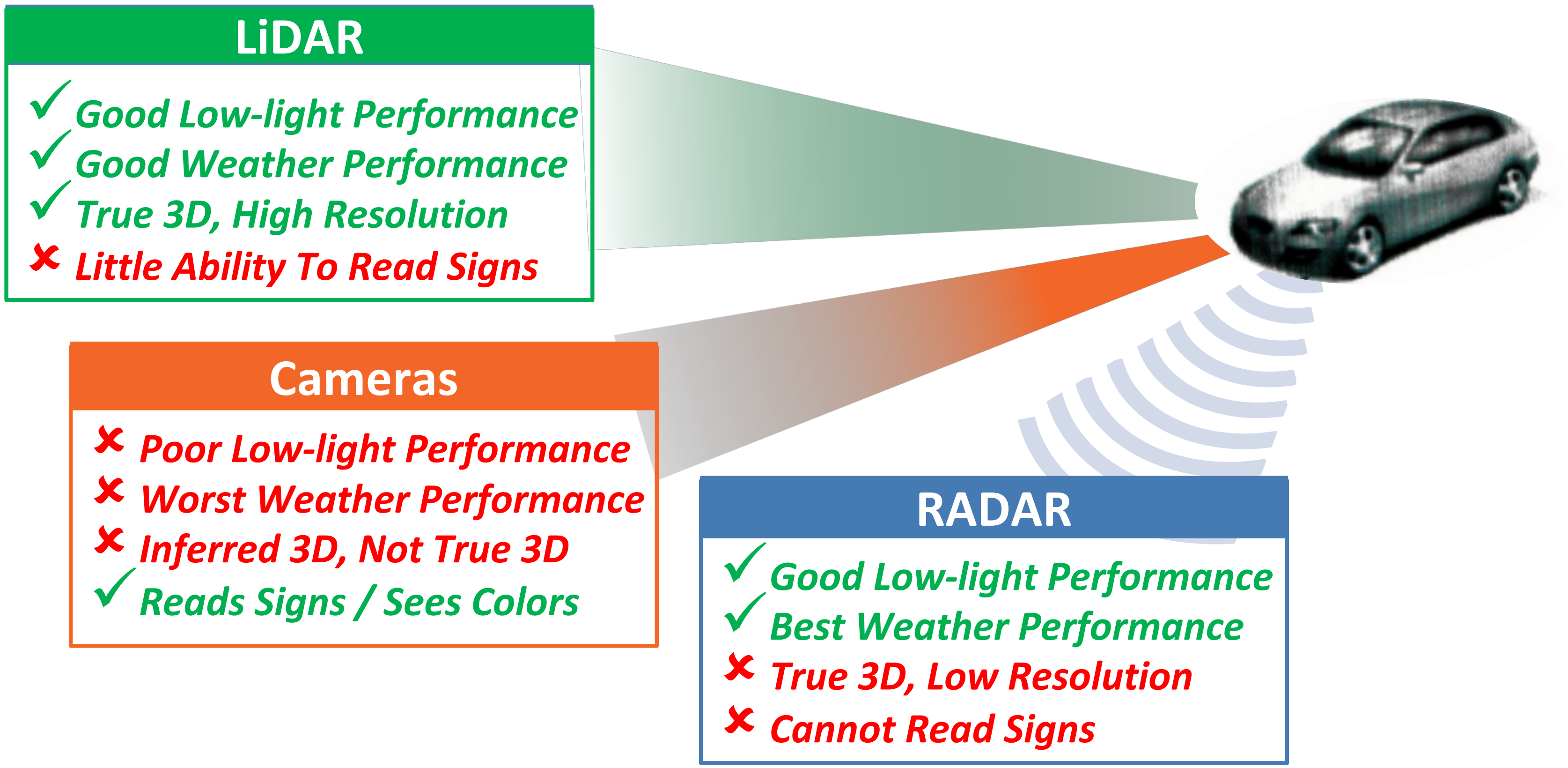

Airborne vs. Automotive LiDAR

Airborne

Automotive

Range

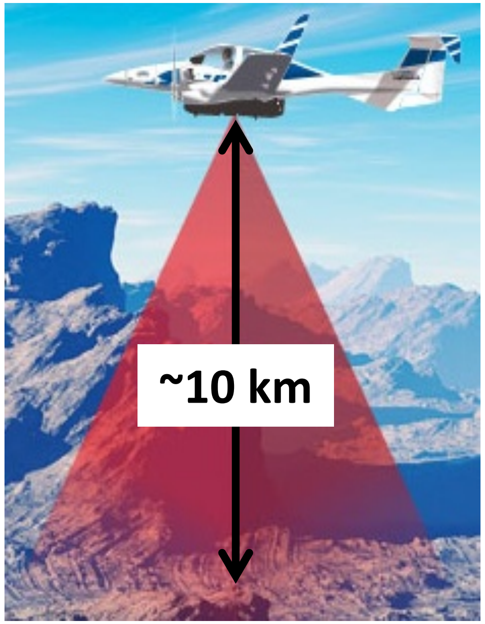

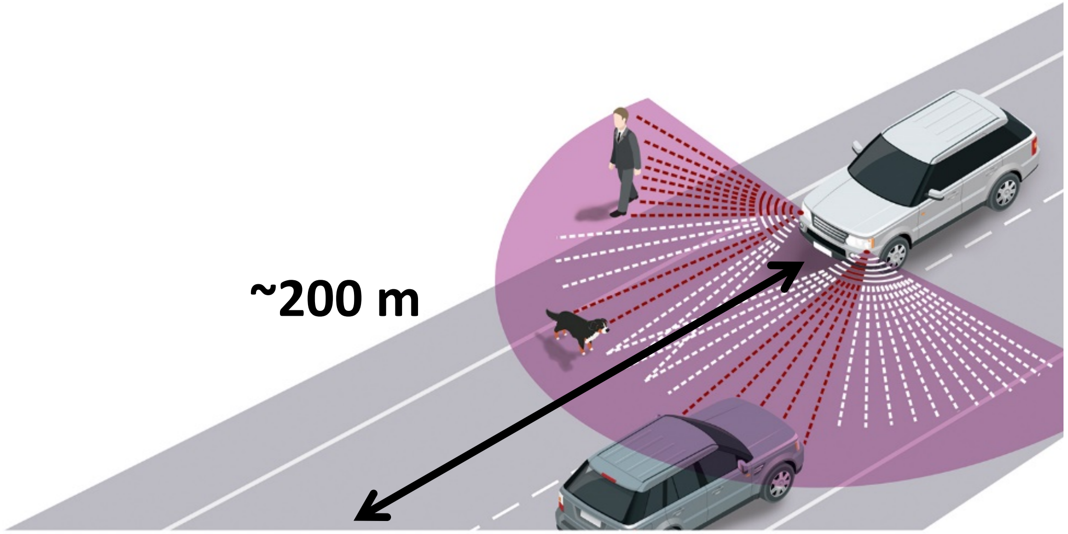

Resolution

Airborne: 2 – 10 pts/m^2

Automotive: 20 – 40 cm resolution at 200 m

Cost

Flash vs. scanning for Auto LiDAR

"Flash" illumination: elegant but impractical for Auto

~100° FOV with 0.1° resolution needs 1000 pixels in one direction → ~Mpixel 2D array

Even given Mpixel array, illuminating all pixels takes prohibitive laser energy

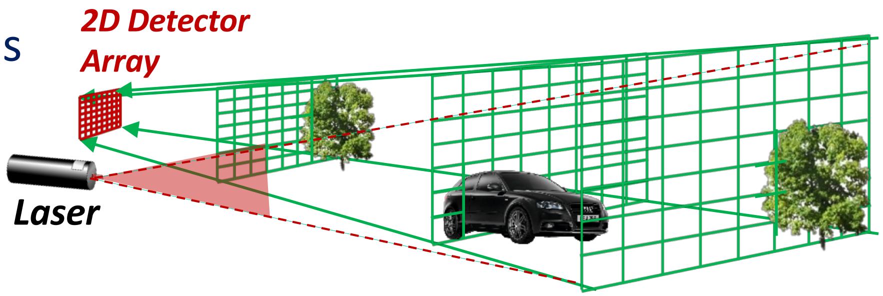

Scanning provides best balance of laser/detector resources

Image vertical FOV with ~1000 pixel 1D array, scan to cover horizontal FOV

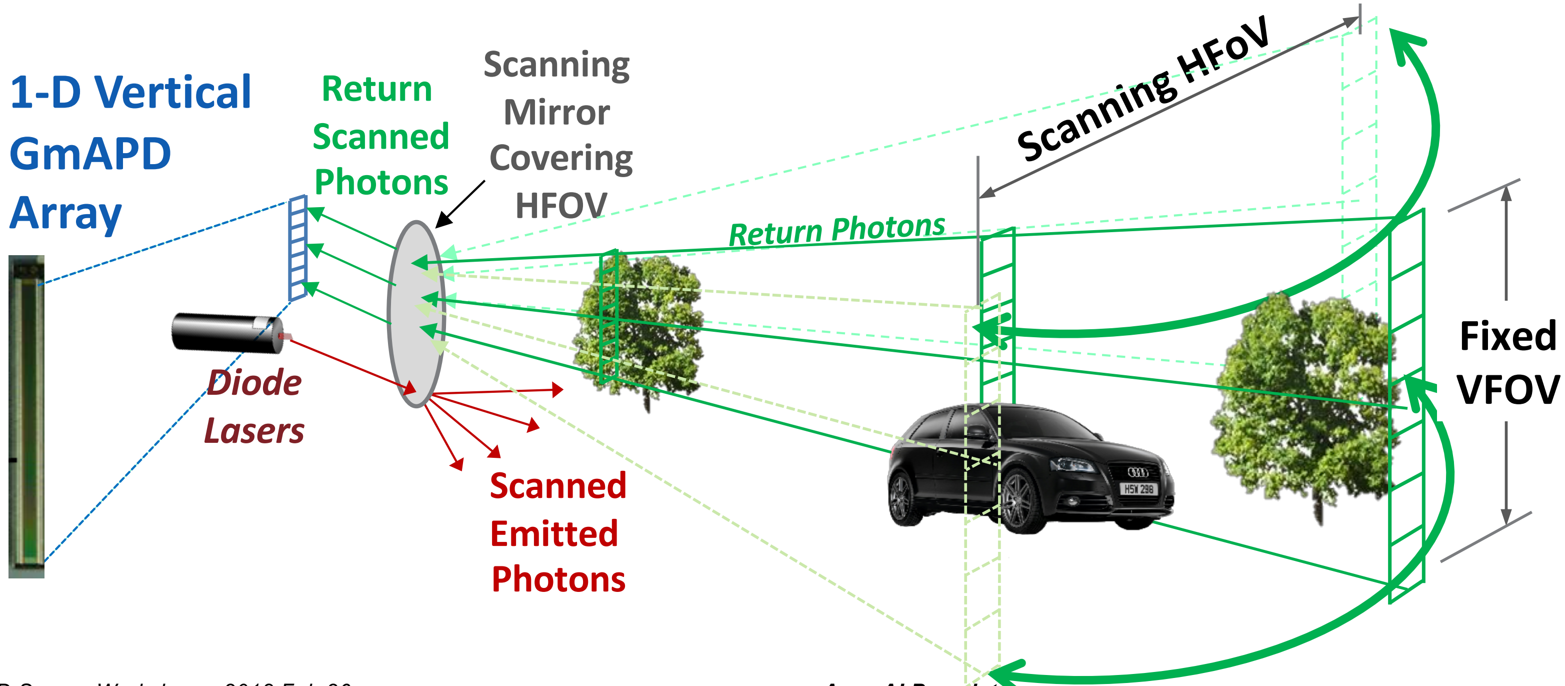

Importance of resolution

0.46°
(8 mrad)

Typical of existing Auto-format LiDAR systems today

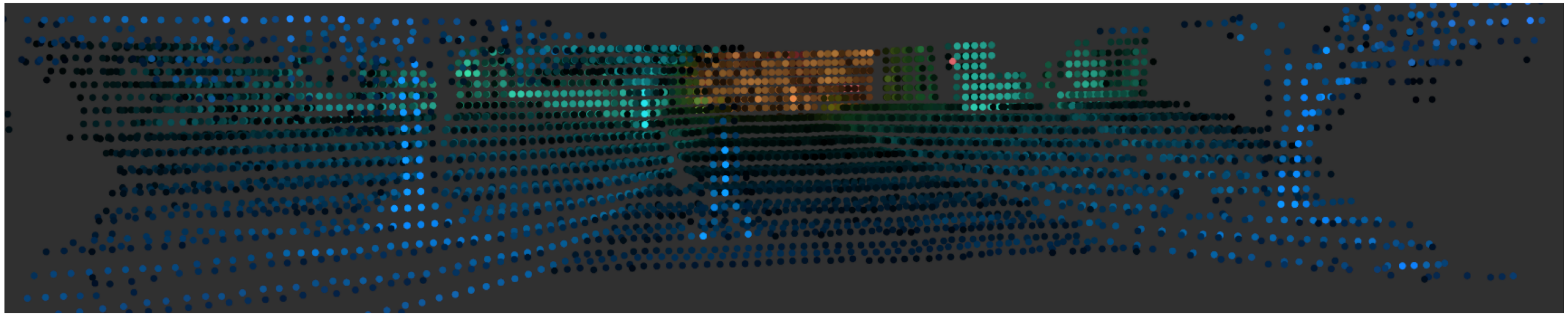

0.23°
(4 mrad)

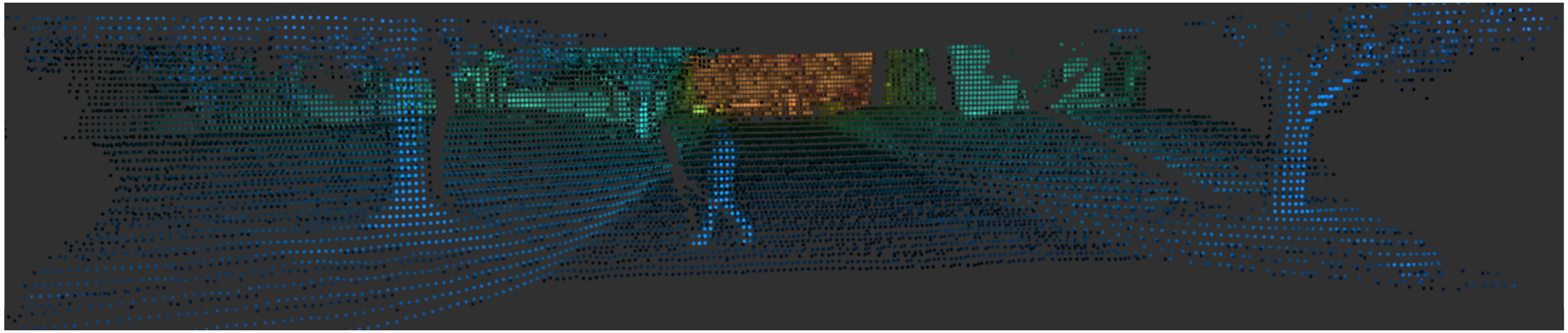

0.057°
(1 mrad)

Capability of Geiger-mode Auto LiDAR in development

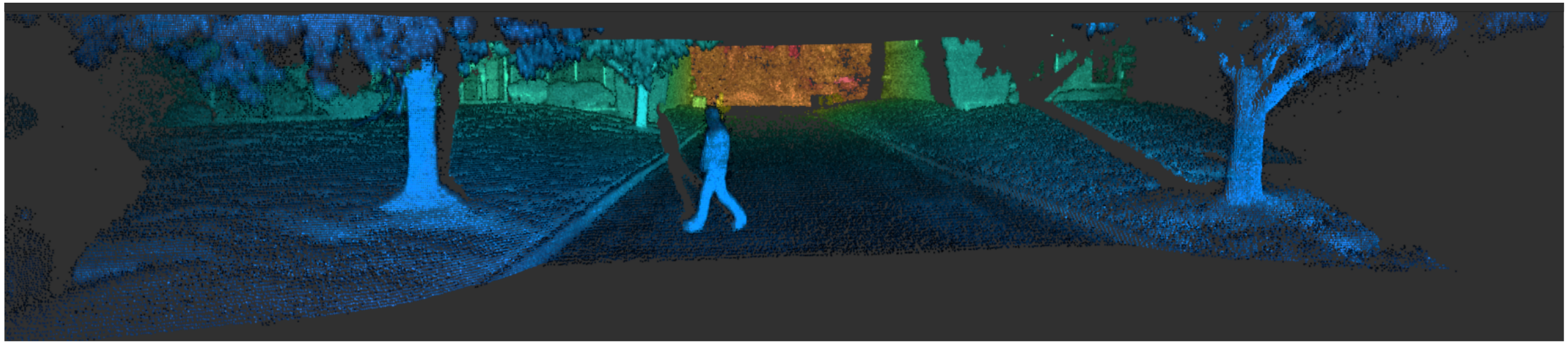

Laser and detector technologies

Fiber laser/solid-state lasers vs. diode lasers

Cost!

Size/weight

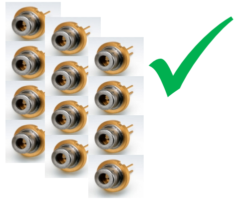

Linear mode detectors vs. Geiger-mode detectors

Transmitter power!

Linear mode needs excessive power for long range, diodes not practical

System size/weight

Auto LiDAR system emulation

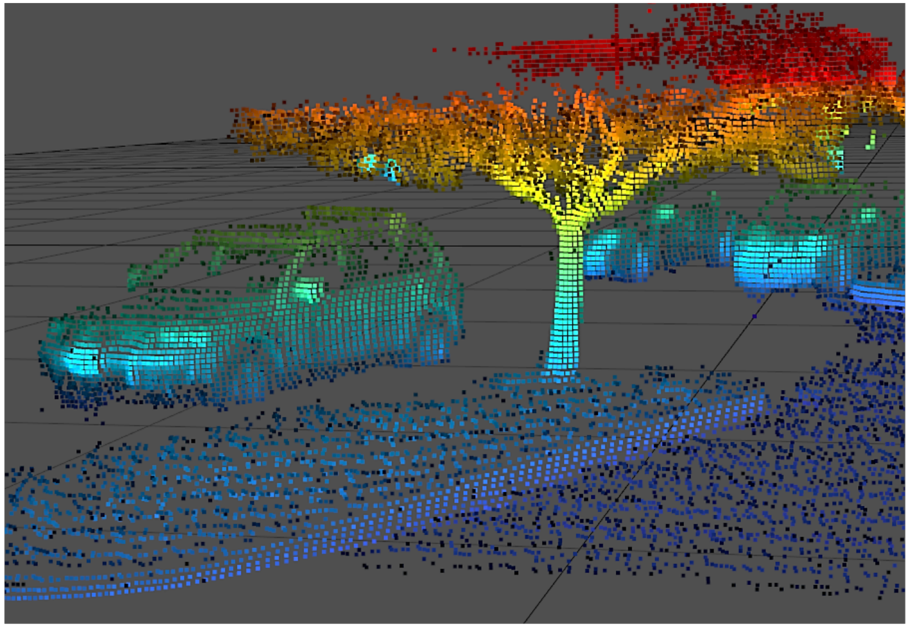

Color-coded for height

Auto LiDAR demonstrator

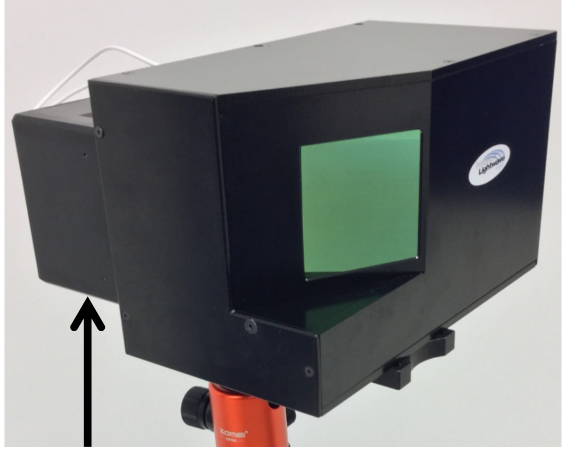

GmAPD 128 x 32 camera

512 x 64 demo 3D point cloud format
Scaling to 2048 x 512 equivalent

Color-coded for distance

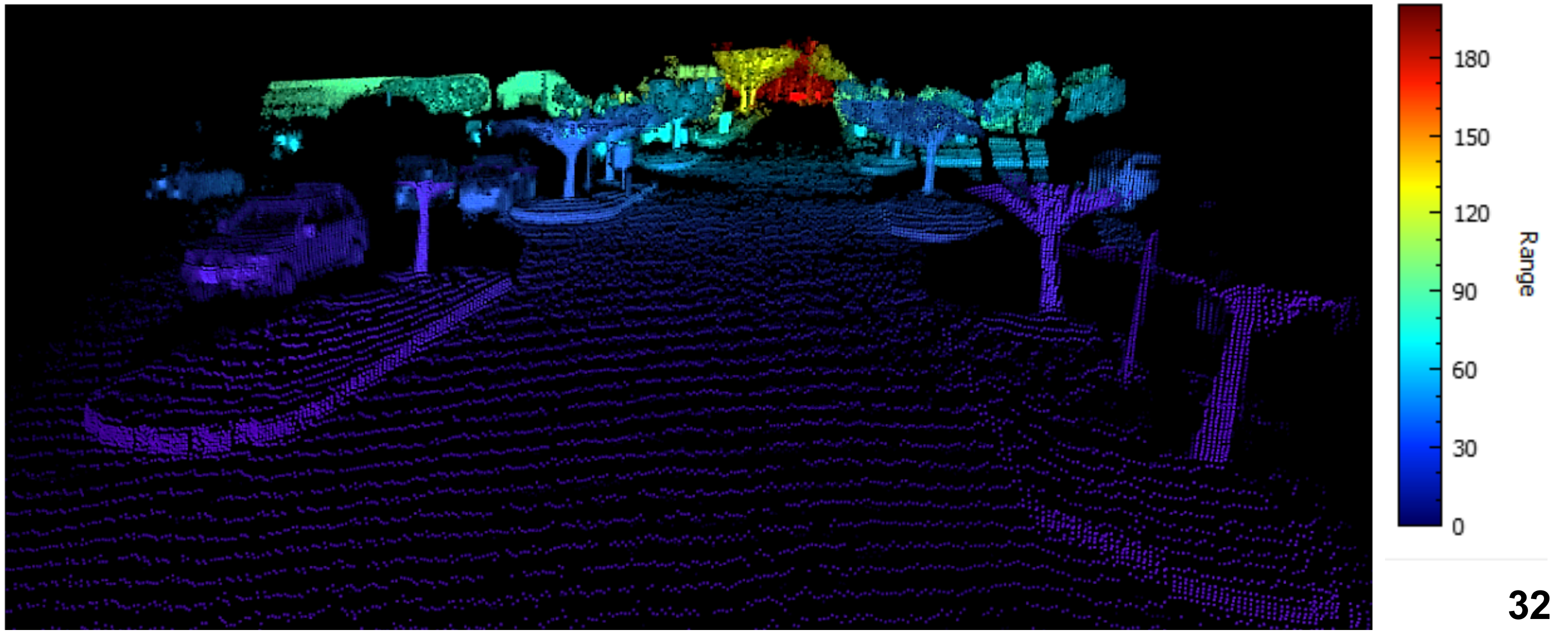

3D driving video imagery with demonstrator

Imagery taken with demonstrator mounted to car roof

Google maps view of 300 m driveway through office park

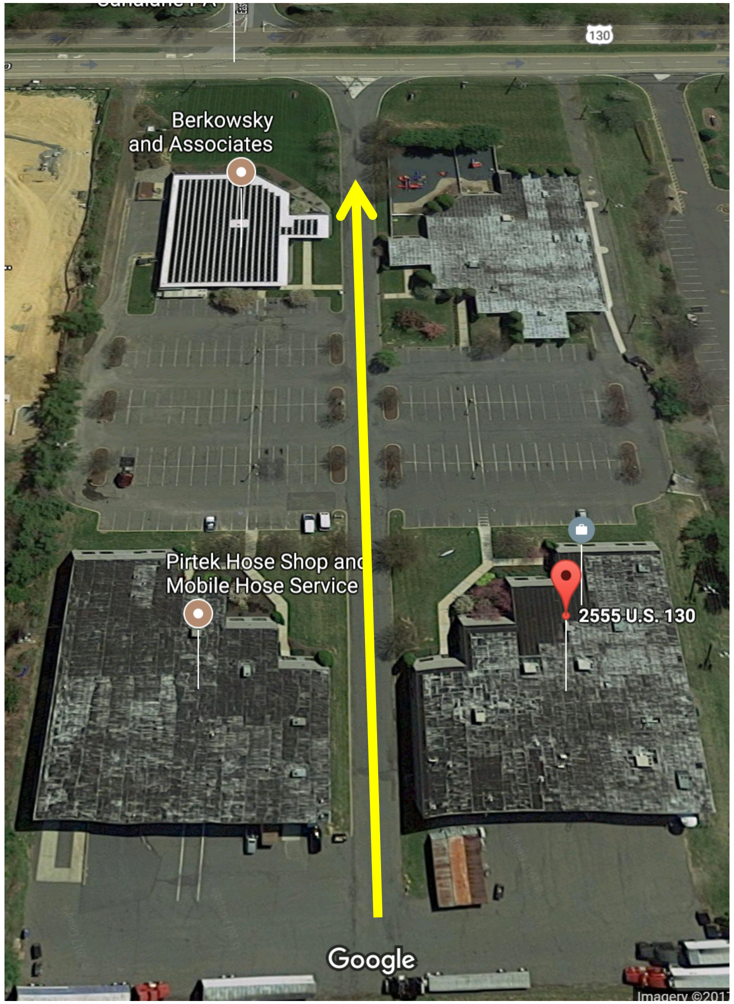

SWIR Geiger-mode technology summary

Initial performance developed for:

Single-photon fiber communications

PDE, DCR, afterpulsing, jitter

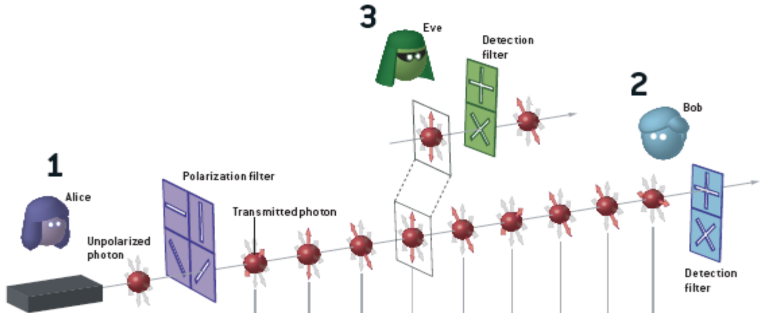

Proven unique capabilities for:

High-altitude 3D LiDAR mapping

Xtalk, array format/yield

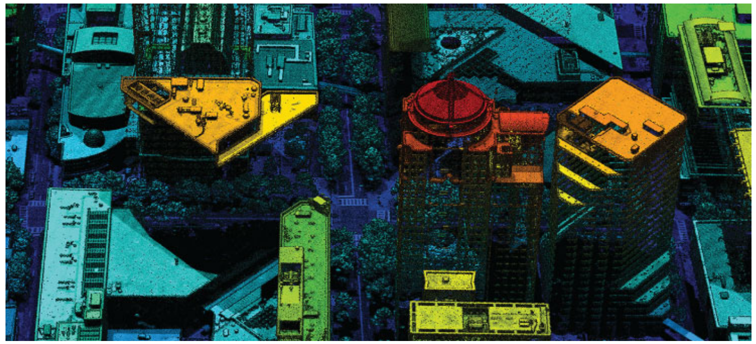

Potential for disruptive impact in:

High-performance automotive LiDAR

range, resolution, SWaP, cost

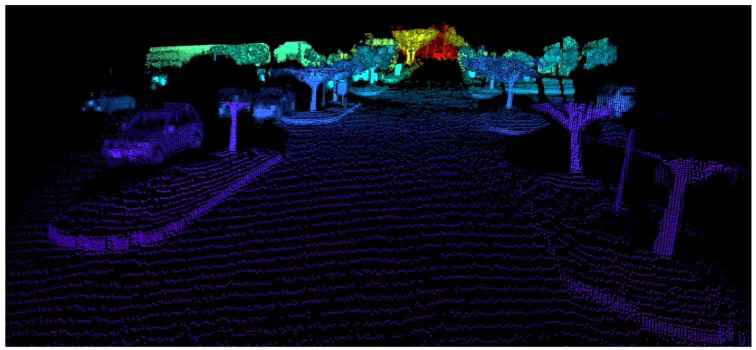

BACK-UP SLIDES

APD I-V Behavior: Linear & Geiger modes

"Linear mode" defines behavior below breakdown voltage V_b

Photocurrent proportional to input optical power → ANALOG

"Geiger mode" operates above V_b with different functionality

Generates macroscopic current pulses → DIGITAL

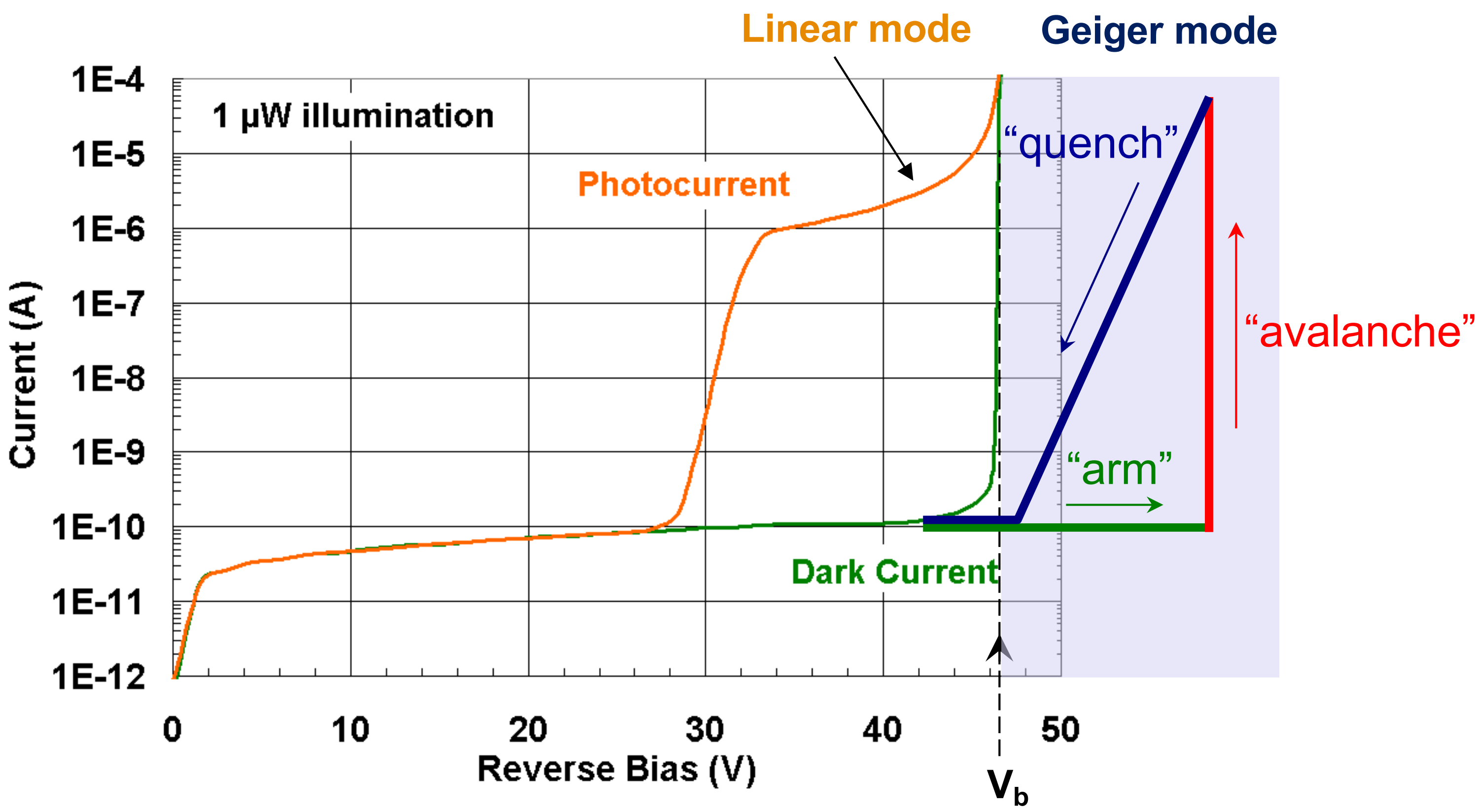

Single-photon detector (SPD) metrics

Photon Detection Efficiency (PDE):
probability that photon arrival causes detector to fire

Dark Count Rate (DCR):
probability that detector fires in absence of photon arrival

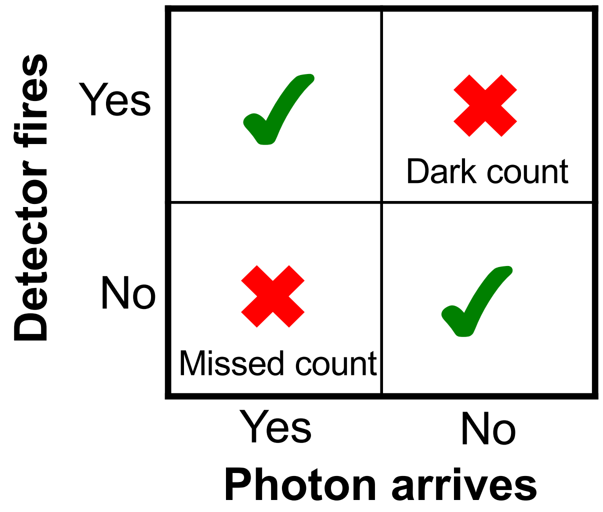

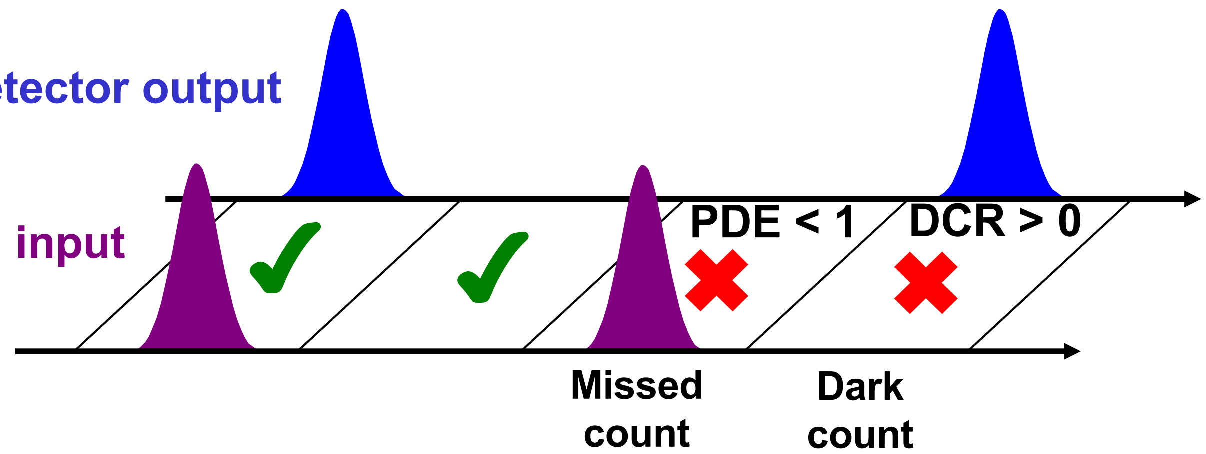

Timing Accuracy: timing uncertainty due to “jitter”

Counting Rate: limited by detector response time and “reset” time

Geiger-mode 3D LiDAR imaging

Geiger-mode for generating 3D imagery (payload)

Disruptive for defense and commercial 3D imaging

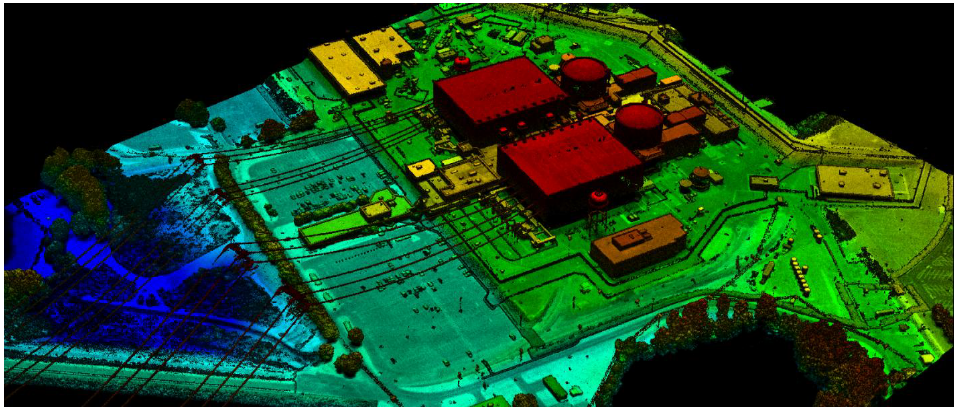

Geiger-mode for autonomous navigation (nav system)

Critical capability for situational awareness and safety functions

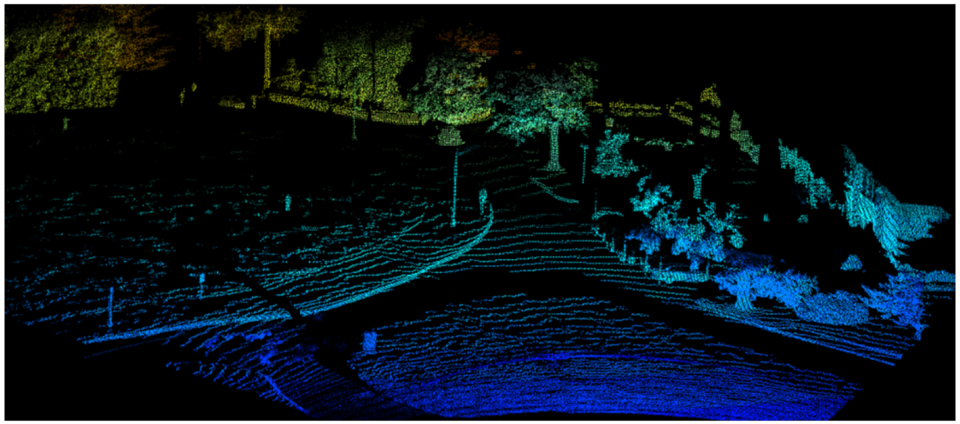

APD operating modes: Linear and Geiger

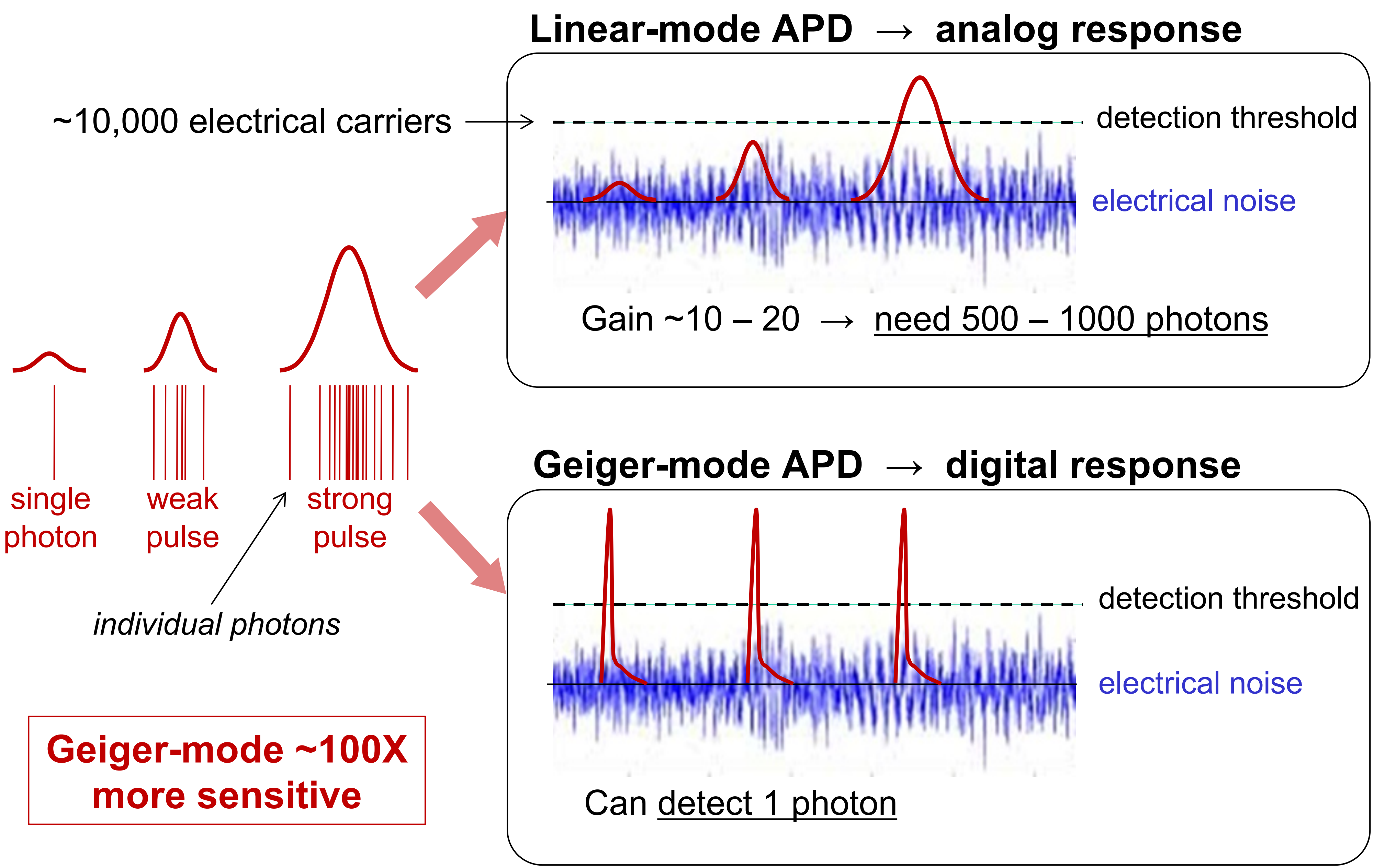

Multi-photon pulse detection efficiency

More photons per return pulse → higher probability of pulse detection

High detection probability (>85%) for ≥5 photons

Optimize LIDAR system design for avg. photons per return pulse

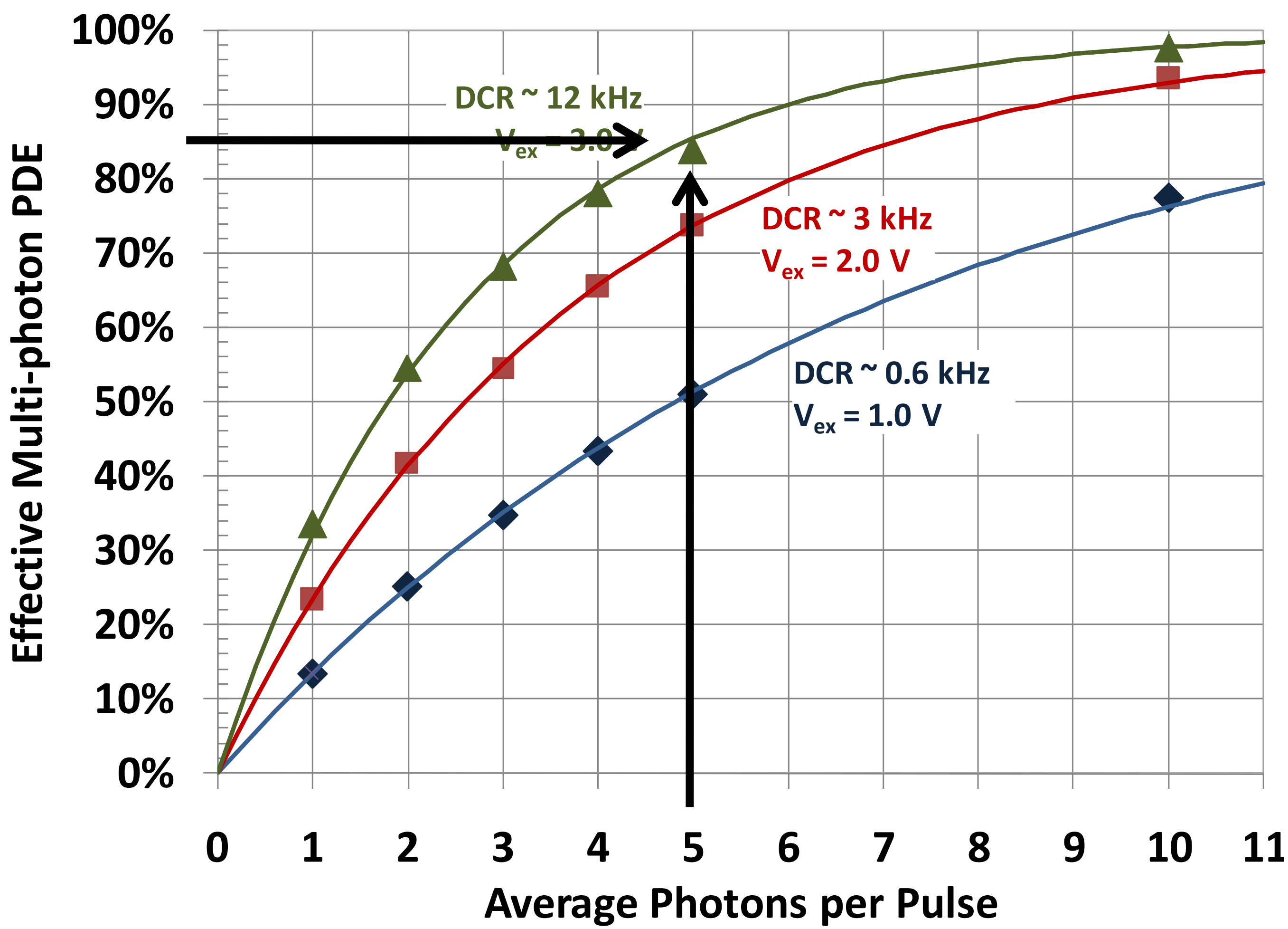

Points:
experimental data

Solid lines:
model

Camera timing accuracy

Short-pulse illumination of entire sensor with η photons per pixel

“Intra-frame” jitter: timing distribution with single frame

“Inter-frame” jitter: timing distribution among successive frames

Broad illumination, short pulse (~100 ps)

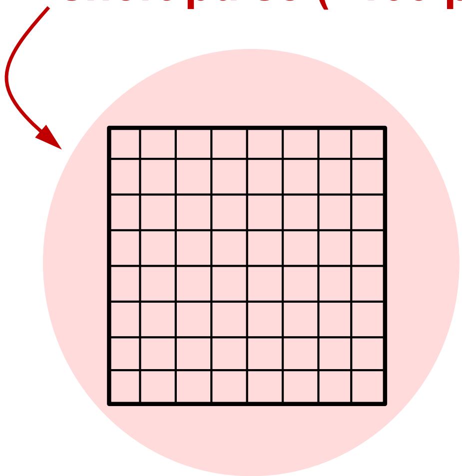

Average of η photons per pixel

“Intra-frame” jitter

Distribution in timing response among all pixels in single frame

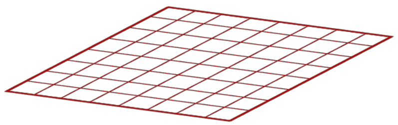

“Inter-frame” jitter

Distribution in timing response for single pixel in successive frames

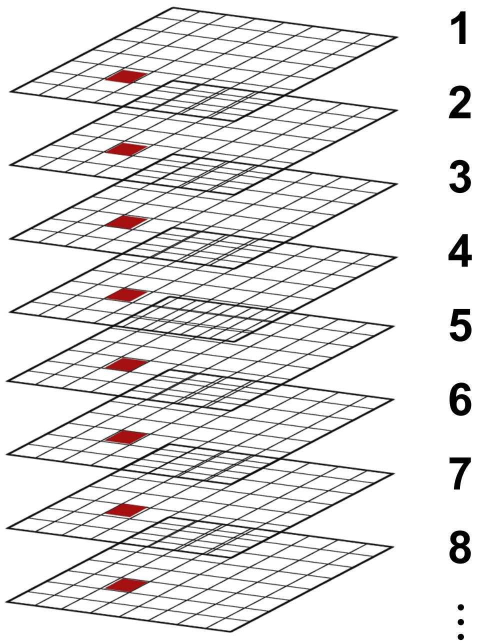

Camera timing jitter

Record arrival times (i.e., time bin) for single frame, multiple frames

2 μs range gate / 250 ps time bins / photon pulse at ~1 μs

rms timing jitter σ ~ 175 ps (includes quantization error) → **~ 2 cm**

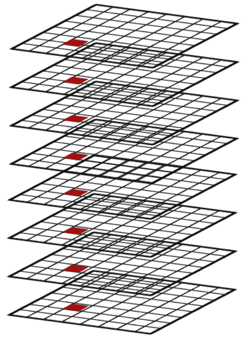

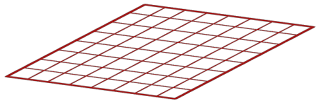

Intra-frame jitter

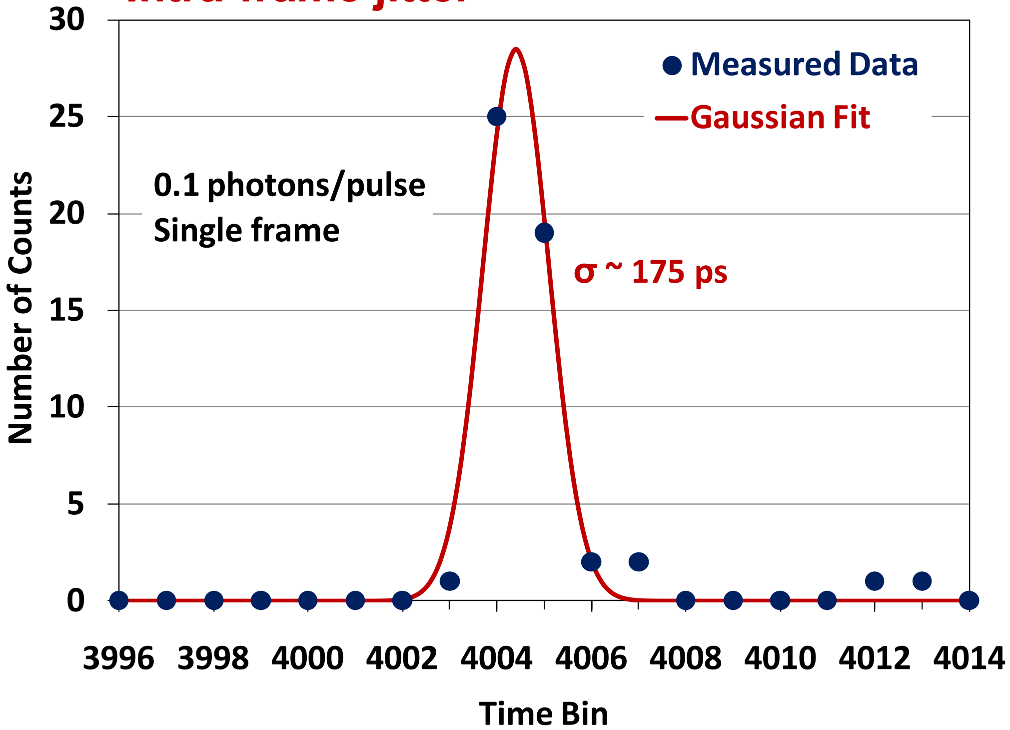

Inter-frame jitter

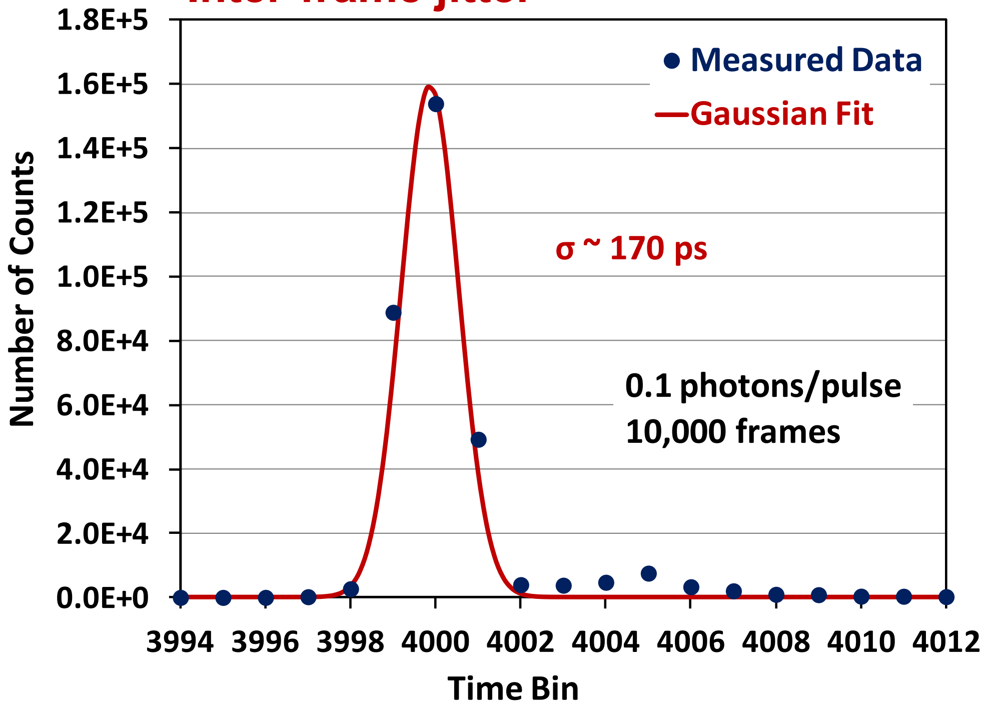

Argo AI Proprietary

Mitigating crosstalk in arrays of GmAPDs

- **Consider optical cross-talk contributions**
  - Avalanches emit crosstalk photons due to hot carrier luminescence
  - Path ① : direct line-of-sight to nearest neighbor pixels
  - Path ② : reflection from back-side surface of PDA
- **Use etched trenches to mitigate line-of-sight crosstalk**

Photo of GmAPD 32 x 32 array

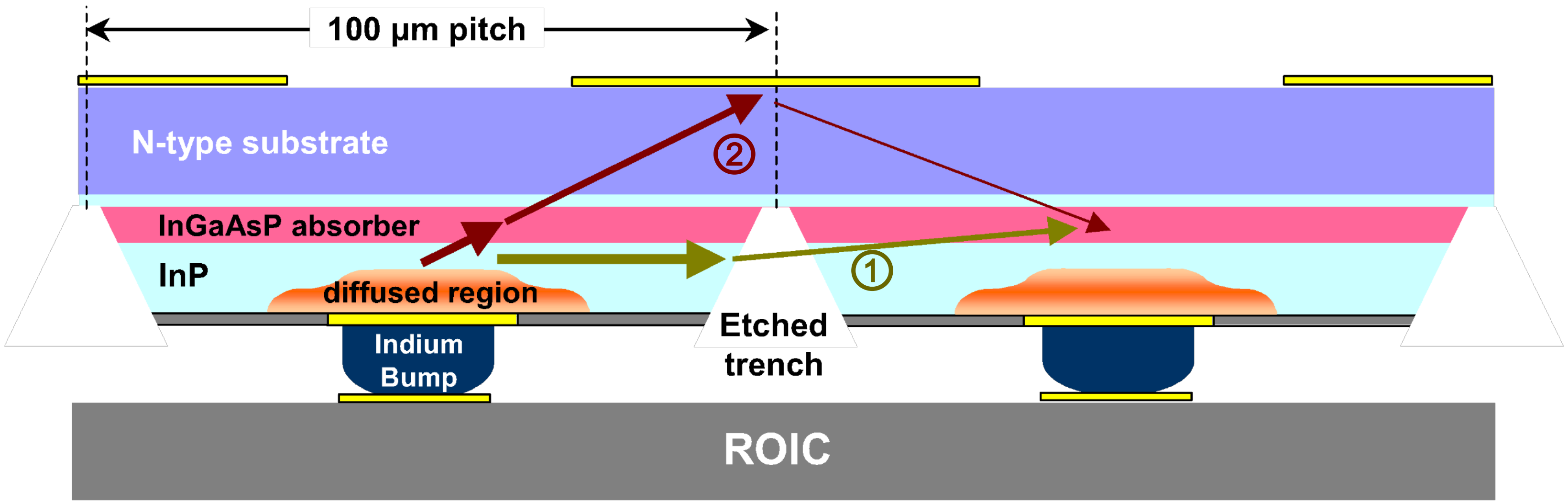

Temporal analysis of Poisson processes

Attributes of a Poisson process (e.g., dark counts, CW Poisson source)

- Memoryless: counts from non-overlapping time intervals are mutually independent
- Probability of count is proportional to time interval Δt (for sufficiently small Δt)
- Probability of more than one count in Δt is negligible (for sufficiently small Δt)

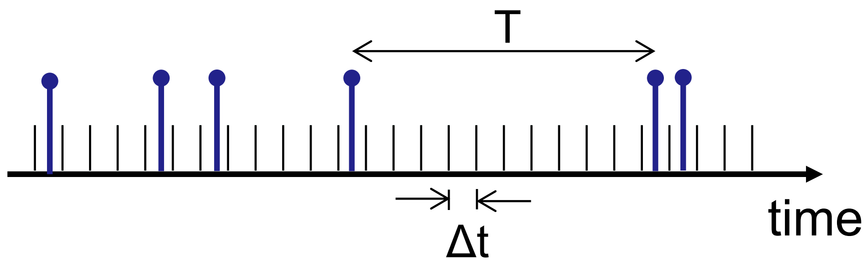

"Inter-arrival" times between successive counts are exponentially distributed

$\rightarrow \; f(T) = \lambda e^{-\lambda T}$

λ = average dark count rate (DCR)

$\int f(T)\, dT = 1$

For group of Poisson processes, collective behavior also exhibits Poisson statistics

Inter-arrival times for dark counts of *all* of pixels of array → Poisson statistics

Deviation from intrinsic DCR Poissonian behavior

- **array-level data: crosstalk**
- **pixel-level data: afterpulsing**

DCR Temporal Analysis: 1.06 µm

- **“Ideal” dark counts can be described as Poisson process**
- **Collection of multiple Poisson processes (all pixels) is a Poisson process**
- **Inter-arrival time distribution from all dark counts should be exponential**
  - Pre-factor and exponent of exponential fit should give DCR

$f(t) = \lambda e^{-\lambda t}$

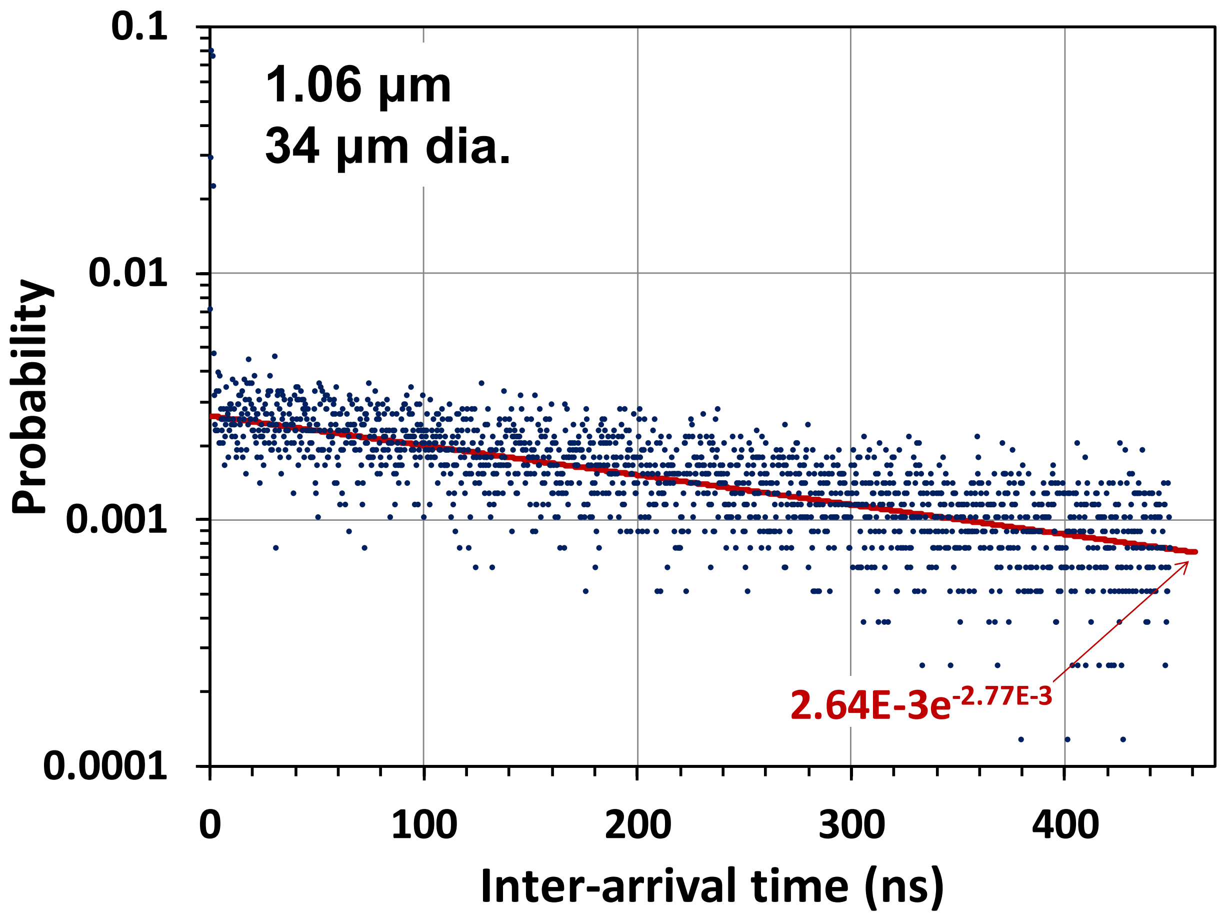

2.64E-3 & 2.77E-3 agree to 5%

~2.7E-3 / ns = 2.7E6 Hz DCR from entire array (1024 pixels)

→ 2.6 kHz DCR per pixel

Agrees with 2.2 kHz DCR mean from array-level DCR map

30% PDE
248 K

Argo AI Proprietary

DCR Temporal Analysis and Crosstalk

- **Assume any non-Poissonian behavior is associated with crosstalk**
- **Sharp peak at 0 to 2 ns inter-arrival time indicates extent of crosstalk**
- **32 x 32 / 34 µm dia. / 100 µm pitch / 1.06 µm wavelength**

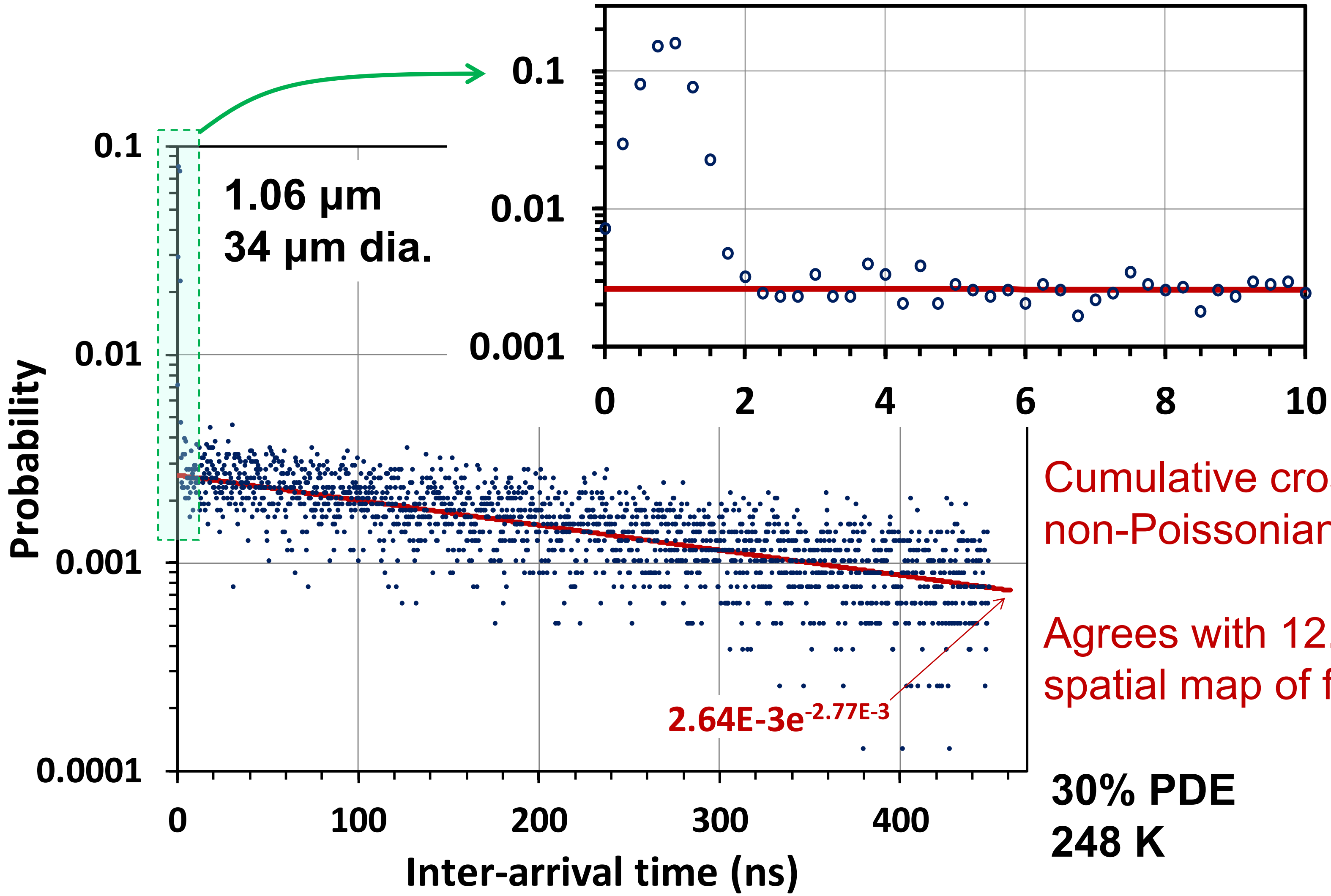

Cumulative crosstalk from non-Poissonian peak is 12.6%

Agrees with 12.2% from spatial map of full 32x32 array

30% PDE
248 K

Crosstalk reduction for smaller detectors

- 32 x 32 / <u>18 µm dia.</u> / 100 µm pitch / 1.06 µm wavelength
- Crosstalk reduced by 12.6%/1.4% ~ 9X for area ratio of $(34\ \mu m/18\ \mu m)^2 \sim 3.6$

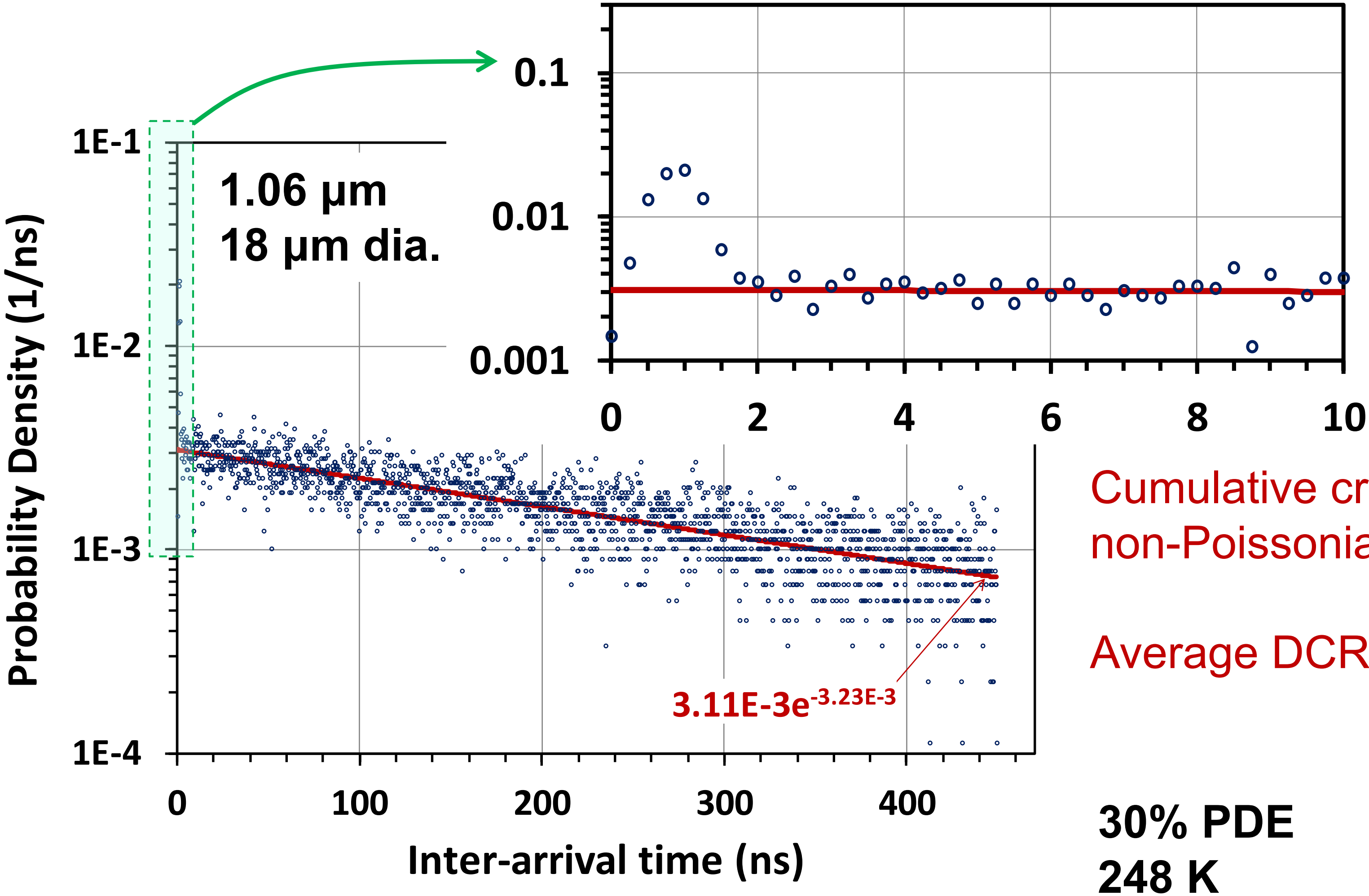

Cumulative crosstalk from non-Poissonian peak is 1.4%

Average DCR = 3.1 kHz

30% PDE
248 K

Crosstalk increase with smaller pitch

- <u>128 x 32</u> / 18 µm dia. / <u>50 µm pitch</u> / 1.06 µm wavelength
- Cumulative crosstalk ~ 34% at PDE = 30%

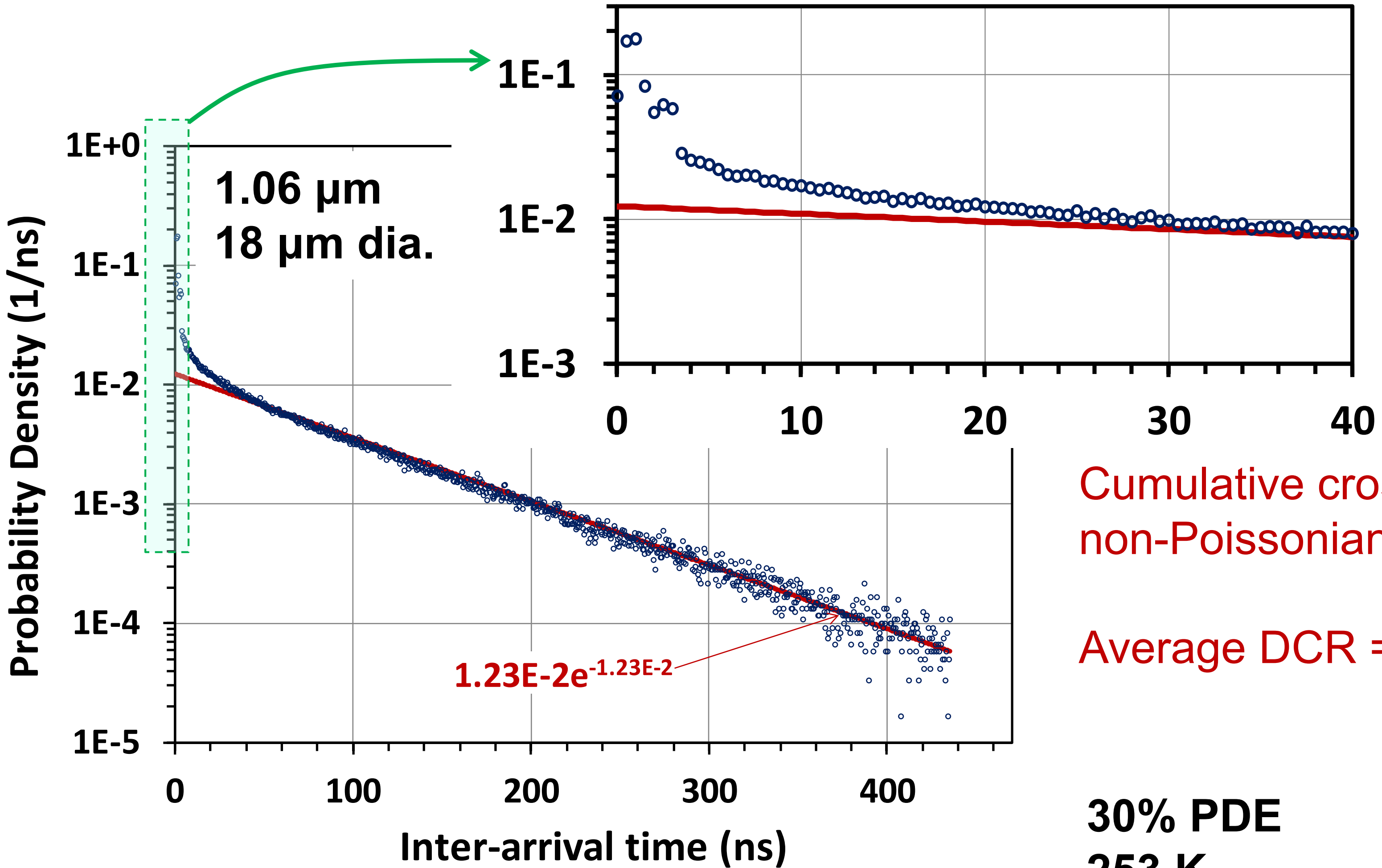

Cumulative crosstalk from non-Poissonian peak is 34%

Average DCR = 3.1 kHz

30% PDE
253 K

Impact of crosstalk on Poisson distribution

- **Larger crosstalk case exhibit "tail" in interarrival time distribution**
  - 128 x 32 / 18 µm dia. / 50 µm pitch / 1.06 µm wavelength
  - Also seen for 32 x 32 array designed for 1.5 µm wavelength
- **Consider effect of crosstalk on Poisson distribution**
  - Crosstalk event divides intrinsic dark count interarrival time T into two segments
  - Crosstalk time T_c and remainder $T' = T - T_c$
  - Replacement of T by T' and T_c changes interarrival time distribution

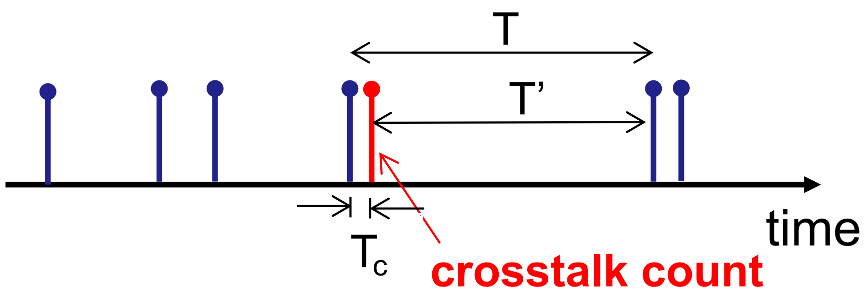

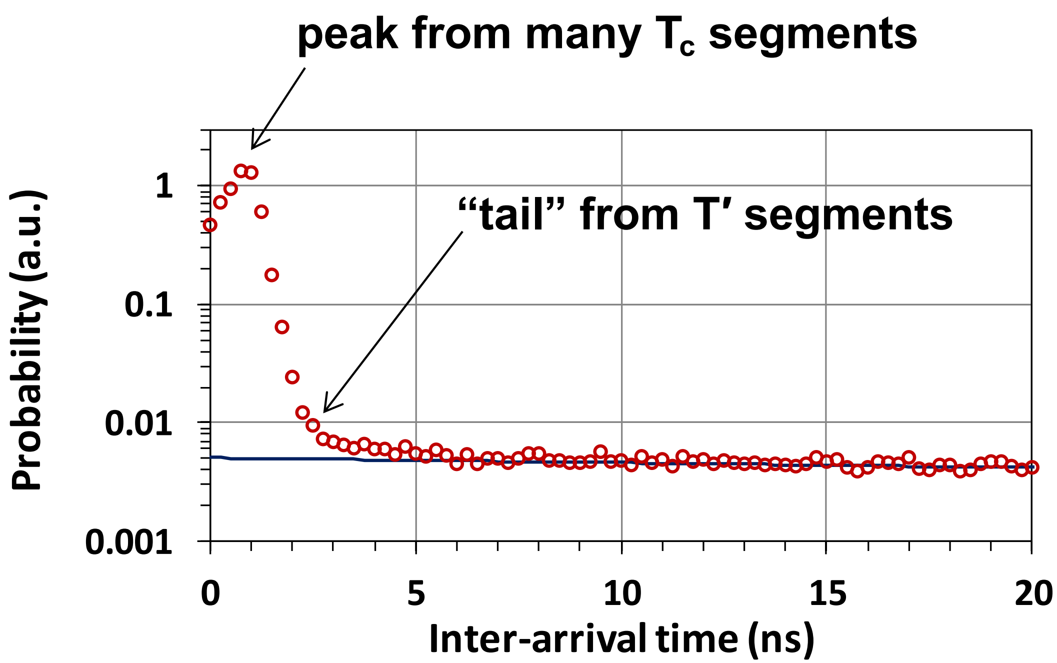

- **Modeling shows "tail" in inter-arrival time distribution**
  - …but requires assumption of much larger cumulative crosstalk
  - Further refinement needed

Next-gen asynchronous GmAPD cameras

Fully free-running (asynchronous) FPAs and cameras

All pixels independently avalanche, quench, and reset

Continuous operation up to 700 Msamples/s

Synchronous → pixels blind until read out

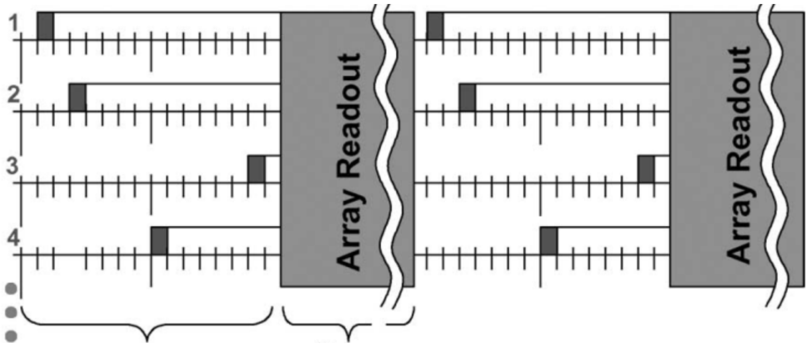

S. Verghese, et al., JSTQE 13, 870 (2007)

Asynchronous → all pixels free-running

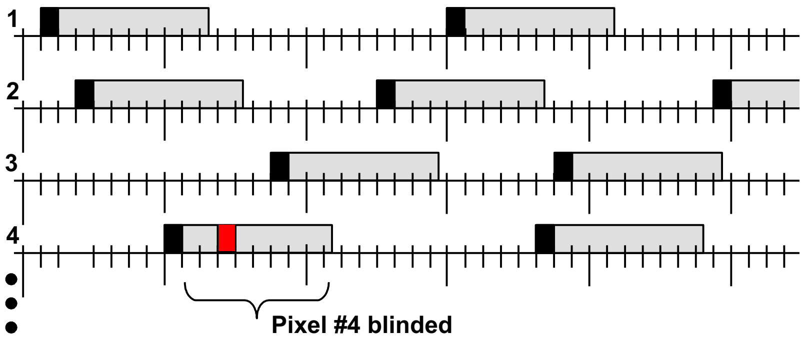

Camera Product	Operation Mode	Format	Pixel Pitch	Pixel Geometry	Sampling Rate	Timing Resolution
Kestrel	synchronous	32 x 32	100 µm	square	200 Mct/s	250 ps
Falcon	synchronous	128 x 32	50 µm	square	400 Mct/s	500 ps → 250 ps
Merlin	asynchronous	32 x 32	66 µm	hexagonal	700 Mct/s	310 ps

Autonomous vehicles

LiDARs produce high-resolution 3D imagery

indispensable for enabling driverless vehicles

see **Small objects**

with **Low reflectance**

at **Long distance**

and **Must be eye-safe!**

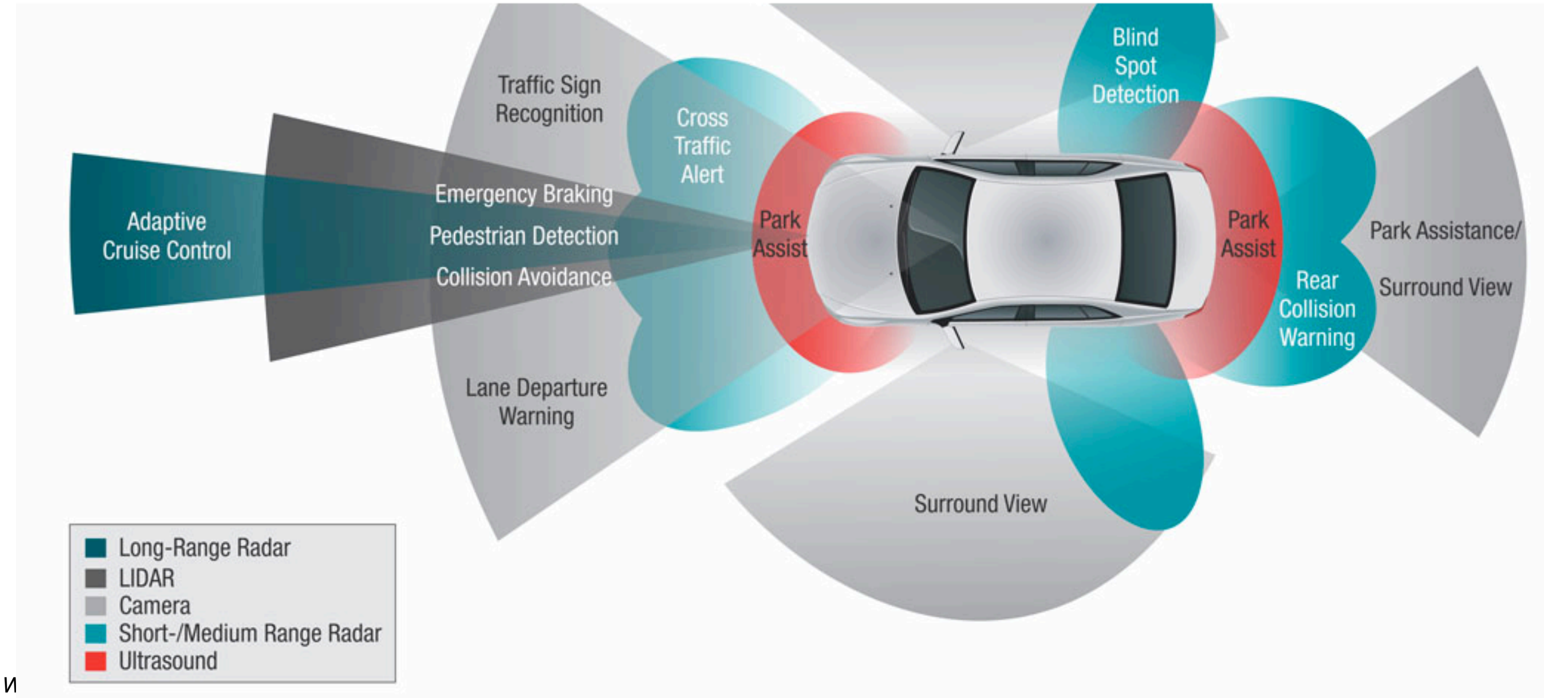

SWIR Geiger-mode benefits for Auto LiDAR

Safer wavelengths

Eye-safety improves by 100,000X above 1400 nm

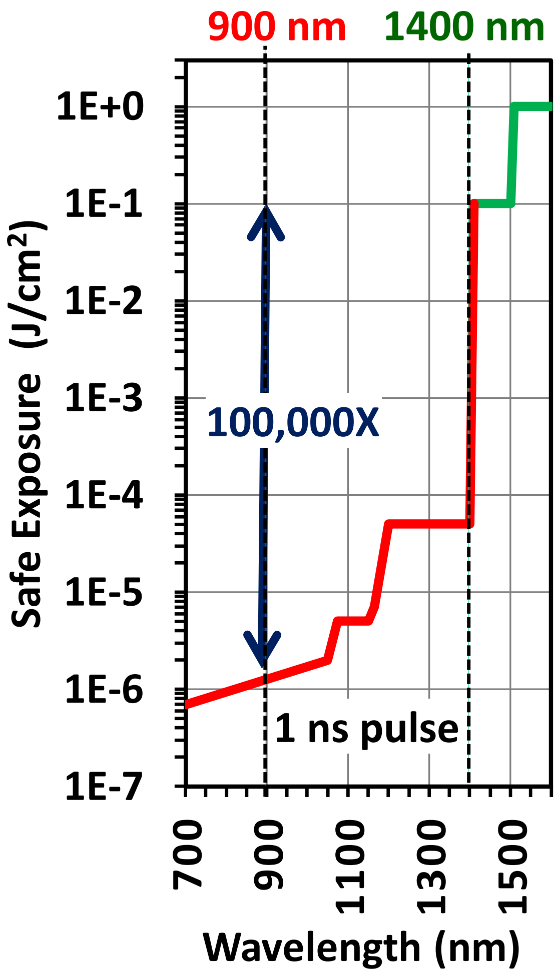

Single-photon sensing

Lower power lasers

Longer distance detection

Efficient use of photons

Legacy detectors: weak optical signals buried in noise

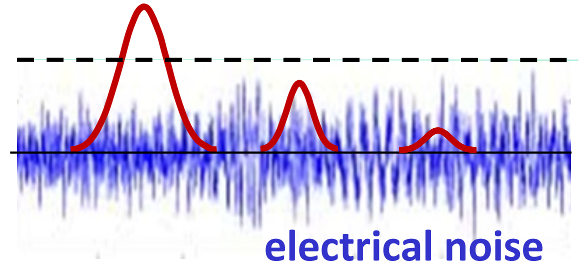

Geiger-mode detectors: easily sense single photons

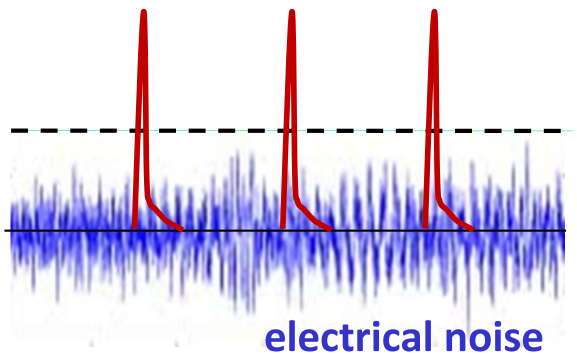

Semiconductor scaling

Key devices in PLI LiDAR:

- Geiger-mode detectors
- Laser diodes

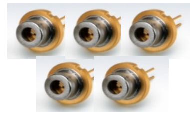

Devices fabricated on semiconductor wafers, meet auto cost targets

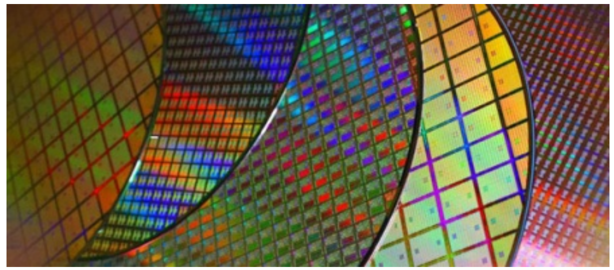

Scanning GmAPD automotive LiDAR

Horizontal scan of 512 x 1 vertical 1-D array

- Long range (>250 m)
- High resolution (0.025° x 0.025°)
- 60° x 15° field-of-view

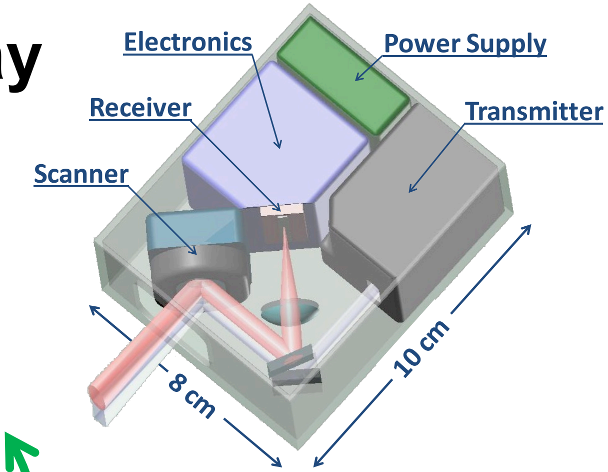

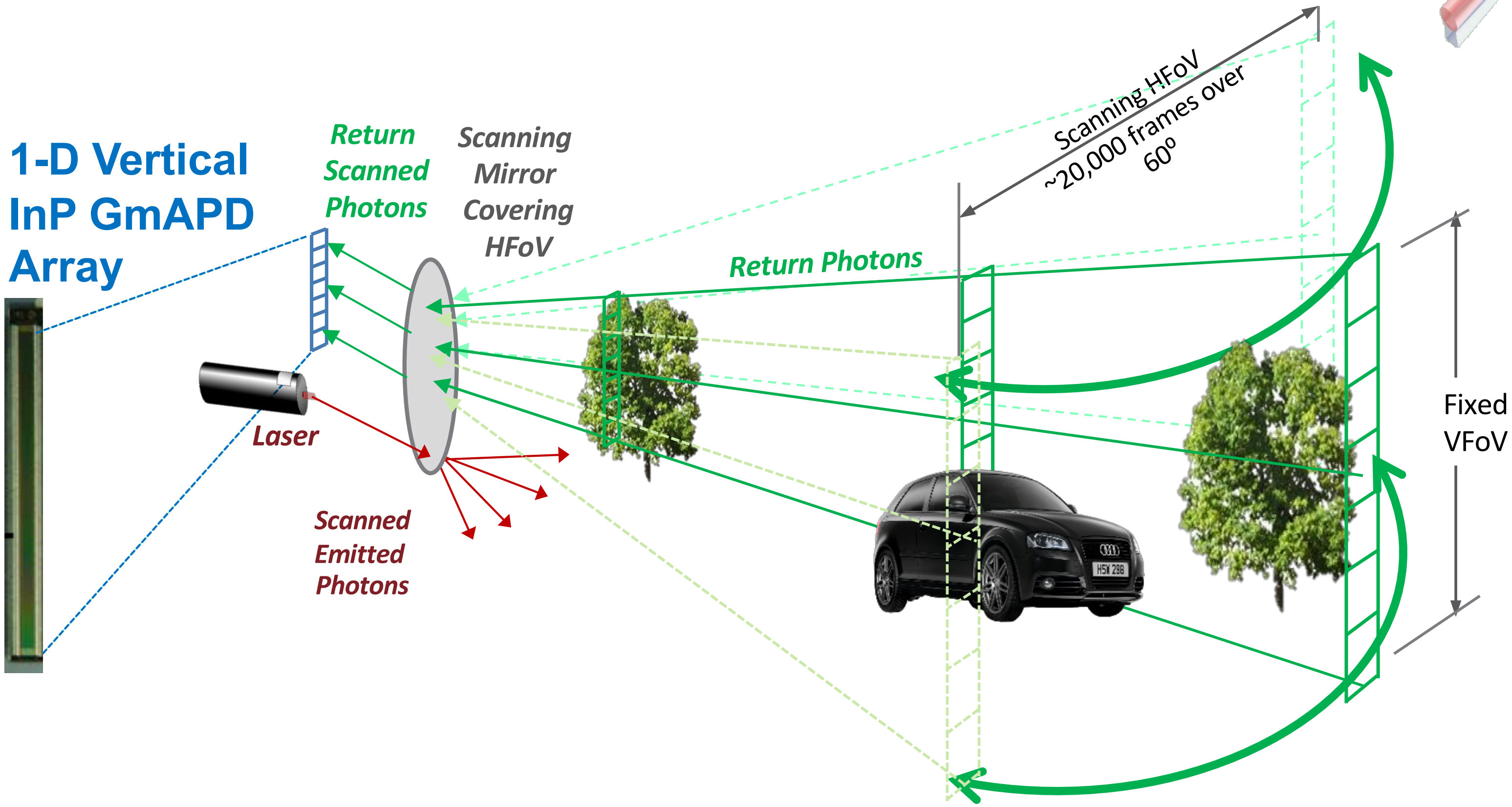

Airborne vs. Automotive LiDAR

LiDAR requirements: Airborne vs. Automotive

Parameter	Airborne	Automotive
Range (10% reflec.)	5 – 15 km	200 – 300 m
Resolution	2 – 20 pts/m^2	~ 100 pts/m^2
Image Rate	n/a	24 Hz
Pixel Field of View	35 µrad (0.0020°)	500 µrad (0.029°)
Eye safety distance	at ~1000 ft.	at aperture (0 ft.)
Sampling rate	~200 Msamples/sec	~200 Msamples/sec
Cost	~$\$10^5 – \$10^6$	~$\$10^2 – \$10^3$

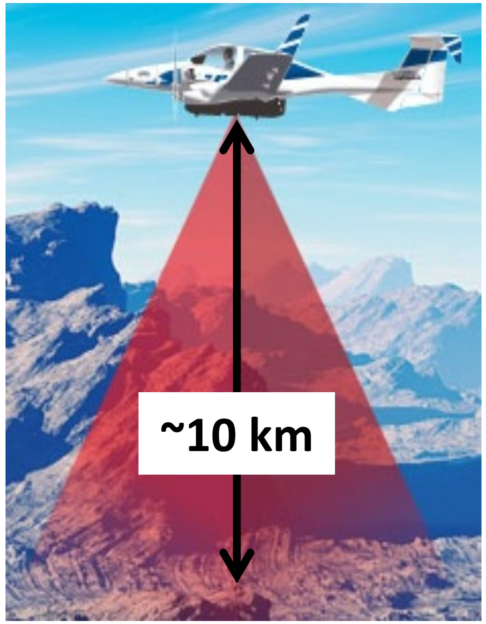

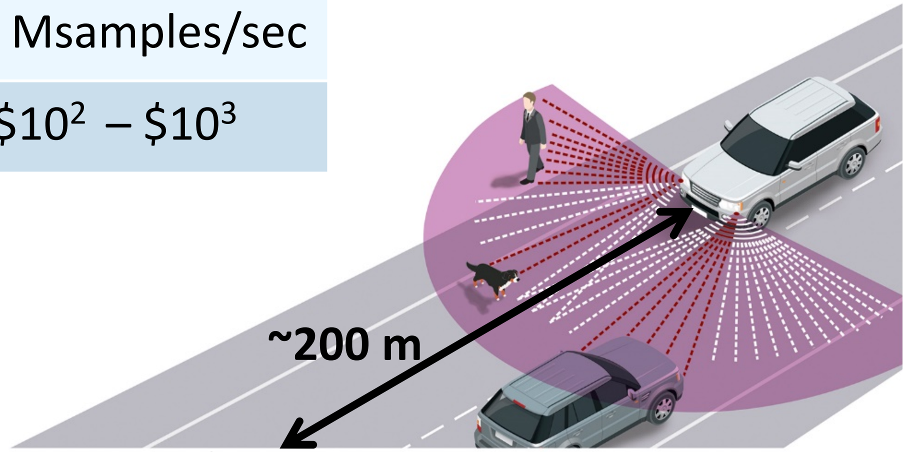

10 cm resolution at 200 m

Auto LiDAR system design

5 major sub-systems

- Transmitter (diode lasers, driver)
- Scanner and optics
- Receiver (GmAPD array, readout circuit)
- Electronics for control and data processing
- Power

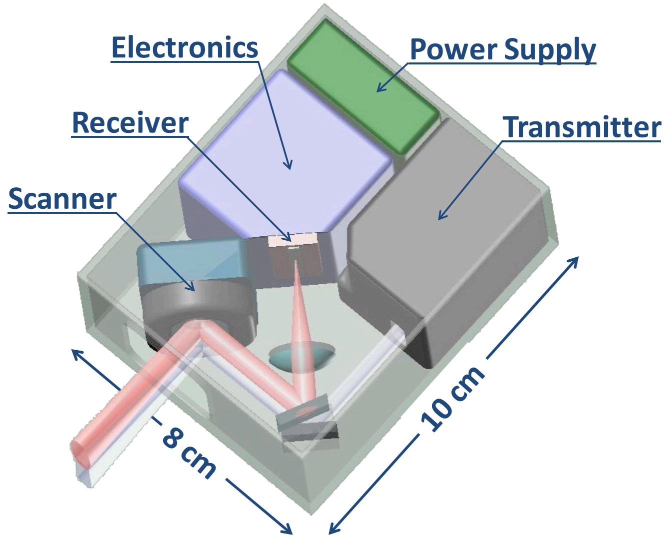

Highly integrated for scalability

- Low cost, low SWaP, and high reliability

Data collection exploits digital nature of Geiger mode

- Statistical approach to filtering noise: "coincidence processing"
  - Eliminates random solar background
- ~100 laser pulses per point cloud point (voxel)
  - ~200 Msamples/sec → ~2M point cloud pts/sec